STRUCTURE EVOLUTION AND RECRYSTALLIZATION IN 7XXX SERIES ALUMINUM ALLOYS

By

JAMESON MARTIN MOORE ROOT

A thesis submitted in partial fulfillment of
the requirements for the degree of

MASTER OF SCIENCE IN MATERIALS SCIENCE AND ENGINEERING

WASHINGTON STATE UNIVERSITY
Department of Mechanical and Materials Engineering

DECEMBER 2010

To the Faculty of Washington State University:

The members of the Committee appointed to examine the thesis of JAMESON MARTIN MOORE ROOT find it satisfactory and recommend that it be accepted.

_____

David P. Field, Ph.D., Chair

_____

David F. Bahr, Ph.D.

_____

Lloyd V. Smith, Ph.D.

ACKNOWLEDGEMENT

The author would like to acknowledge Kaiser Aluminum for funding this research. Special thanks to Mory Shaarbaf, Steven Long, Paul Ainsworth, and Rick Anderson at Kaiser Aluminum for their assistance with the project, including providing direction for the work as well as assistance with etching and optical analysis of the plane strain experiments. Additionally, the author would like to acknowledge Hamid Azizi, Fateh Fazeli, and Dr. Warren Poole at the University of British Colombia in Vancouver, BC for providing access to the Gleeble 3500 testing machine and their assistance in performing the uniaxial deformation experiments.

STRUCTURE EVOLUTION AND RECRYSTALLIZATION IN

7XXX SERIES ALUMINUM ALLOYS

Abstract

by Jameson Martin Moore Root, M.S.
Washington State University
December 2010

Chair: David P. Field

Hot rolling is an important thermomechanical processing technique used extensively in industrial metal production. Aluminum alloys are a common structural material and are generally hot rolled in the process of converting a cast metal ingot into a final or near-final structure. Hot rolling of aluminum leads to a complex deformed structure with inhomogeneous distribution of solute elements, second phase particles, and recrystallization.

Recrystallization is the process whereby new, strain-free grains nucleate from a deformed structure and grow. Recrystallization is an important feature of hot-rolled products as recrystallized grains decrease mechanical properties. Particularly for applications using an as-rolled alloy, or machined from a single hot-rolled plate, controlling recrystallization is a critical concern in industrial thermomechanical processing with major economic implications.

Improved understanding of the hot-rolling process through modeling can help optimize industrial practices. The purpose of this study was to perform experiments simulating hot rolling deformation—providing insight into conditions present during hot rolling relative to thermomechanical processing parameters. Results from this experiment will be utilized in a framework of a through-process hot rolling model.

TABLE OF CONTENTS

Page

ACKNOWLEDGEMENTS iii

ABSTRACT iv

LIST OF TABLES vii

LIST OF FIGURES viii

CHAPTER

1. INTRODUCTION 1

1.1 THERMOMECHANICAL PROCESSING 1

1.2 PROCESSING STAGES 2

1.2.1 CASTING 3

1.2.2 HOMOGENIZATION 3

1.2.3.1 HOT ROLLING 4

1.2.3.2 HOT ROLLED STRUCTURE 6

1.2.4 SOLUTIONIZING 7

1.2.5 AGING 8

1.3 ANNEALING 8

1.3.1 RECOVERY 9

1.3.2.1 RECRYSTALLIZATION 10

1.3.2.2 RECRYSTALLIZATION KINETICS 11

1.3.2.3 PARTICLE STIMULATED NUCLEATION 12

1.3.2.4 DYNAMIC AND STATIC RECRYSTALLIZATION 13

1.3.2.5 RECRYSTALLIZATION INHIBITORS 14

1.3.2.6 GRAIN GROWTH 16

1.3.2.7 RECRYSTALLIZATION TEXTURES 17

TABLE OF CONTENTS (CONTINUED)

Page

1.4 DEFORMATION TEXTURES 17

1.5 PLANE STRAIN TESTING 18

2. RESEARCH DESIGN AND METHODOLOGY 19

2.1 UNIAXIAL DEFORMATION EXPERIMENTS 19

2.2 PLANE STRAIN EXPERIMENTS 20

2.3 HEAT TREATMENT 24

2.4 METALLOGRAPHY 25

CHAPTER TWO FIGURES 26

3. ANALYSIS 28

3.1 UNIAXIAL DEFORMATION ANALYSIS 28

3.2 UNIAXIAL DEFORMATION RESULTS 28

3.2.1 RECRYSTALLIZATION AND STRAIN 29

3.2.2 RECRYSTALLIZATION AND DEFORMATION TEMPERATURE 29

3.3 PLANE STRAIN ANALYSIS 30

3.4 PLANE STRAIN RESULTS 30

3.4.1 RECRYSTALLIZATION AND STRAIN 30

3.4.2 RECRYSTALLIZATION AND STRAIN RATE 31

3.4.3 RECRYSTALLIZATION AND DEFORMATION TEMPERATURE 31

3.4.4 RECRYSTALLIZATION AND ANNEALING TIME 32

CHAPTER THREE FIGURES 34

4. CONCLUSIONS 43

BIBLIOGRAPHY 45

LIST OF TABLES

Page

Table 2.1: Uniaxial test conditions 20

Table 2.2: Plane strain test conditions 22

Table 3.2: Uniaxial test results 29

Table 3.4.4: Plane strain test results 33

LIST OF FIGURES

Page

Figure 2.2: Plane strain ram configuration 26

Figure 2.3.1: Coordinate axes for the plane strain specimen 27

Figure 2.3.2: Plane strain specimen sectioned for heat treatment 27

Figure 3.1.1: Identified features of recrystallized structure 34

Figure 3.1.2: Recrystallization analysis 35

Figure 3.2.1: Recrystallization as a function of strain rate (uniaxial) 35

Figure 3.2.2: Recrystallization as a function of deformation temperature (uniaxial) 36

Figure 3.4.1: Recrystallization as a function of strain (plane strain) 36

Figure 3.4.2.1: Recrystallization as a function of strain rate (plane strain) 38

Figure 3.4.2.2: Recrystallization with increasing strain rate (plane strain) 39

Figure 3.4.3.1: Recrystallization as a function of deformation temperature (plane strain) 40

Figure 3.4.3.2: Recrystallization with increasing deformation temperature (plane strain) 41

Figure 3.4.4 Recrystallization as a function of annealing time (plane strain) 41

CHAPTER ONE

INTRODUCTION

1.1 THERMOMECHANICAL PROCESSING

Thermomechanical processes, such as hot rolling, extrusion, and forging, are common industrial practices to produce final metal products from ingots with the desired mechanical and microstructural properties. Processes like hot rolling are capable of optimizing microstructures in many alloys, including aluminum. Aluminum alloys are commonly used in aerospace applications such as fuselage, wing, and support structures due to low density and good mechanical properties [1-8]. Aluminum is also used in land and marine vehicles as well as food containers and other structural applications [1, 9]. Heat-treatable alloys like 7xxx series (primary alloying elements: zinc, magnesium, and copper) are particularly desirable for aerospace applications as they develop high specific strength [6, 8]. These aluminum alloys generally undergo thermomechanical processing in their production.

A single hot-rolled plate of aluminum can be used for large components like the wing spar of a plane, or machined into complex components, but reliable production requires sufficiently uniform microstructure throughout the plate [2, 8, 10]. Controlling the microstructure and texture of aluminum during thermomechanical processing is crucial for industrial metal production [6, 11, 12]. The effects of thermomechanical processing parameters—deformation temperature, strain rate—on the final material properties are of particular interest [1, 3].

Mechanical properties of a metal are influenced by its microstructure [1, 2, 4, 13]. A uniform, fine final microstructure is generally desired for low-temperature, high-strength applications. However, the structure of hot-rolled metals varies significantly throughout thick

plates. Grain size, crystallographic texture, solute concentration, particle size and distribution, and recrystallized fraction can vary greatly through the thickness of the plate [8, 10, 11].

Recrystallization can occur during hot rolling and is important in determining the final structure and properties of metal [2, 13]. Recrystallization decreases strength and toughness and can reduce corrosion resistance of aged alloys [7]. A low volume fraction of recrystallization is necessary for structural applications requiring high strength [13]. Due to variation in solute and dispersoid concentration, particle size and distribution, deformation conditions, quench rates, and temperature, recrystallization varies throughout the structure of hot-rolled thick aluminum plates [8, 10, 12, 14-16].

Optimizing hot deformation processes is necessary to meet commercial and industrial needs. Investigations of commercial hot-working processes can be difficult due to the size of components and high temperatures. Additionally, during hot deformation, strain rate and deformation continuously change [17]. Modeling deformation processes can aid in understanding the structure and deformation conditions throughout thermomechanical processing [18, 19].

1.2 PROCESSING STAGES

Typical industrial processing for hot-treatable aluminum, including 7xxx series, consists of several stages. The metal goes through casting, homogenization, preheat, hot rolling, solutionizing and quenching, and aging [7, 8, 13, 20]. Casting and homogenization are of particular interest as these stages are important in determining the microstructure evolution in the subsequent processing [21].

1.2.1 CASTING

Cast alloys form a segregated structure when they solidify, including redistribution of solute elements and an inhomogeneous microstructure [8, 22]. The chill zone at the ingot surface consists of randomly distributed grains, rapidly cooled during solidification. Farther from the surface, the structure consists of columnar grains aligned with the direction of heat transfer. The center of the cast is comprised of equiaxed grains [22]. Dispersoids like Al_3Zr that precipitate from this structure therefore have an inhomogeneous distribution in subsequent stages [14, 15]. Features of the cast structure that influence workability include the solidification structure, second phases present, and grain size [22].

1.2.2 HOMOGENIZATION

Prior to rolling, the metal is heated to the homogenization temperature and held to produce a structure in the ingot as homogeneous as possible. Hot deformation of a homogenized ingot structure is less difficult than for an ingot that has not been homogenized. Homogenization also improves surface quality of the final hot-rolled product [22]. Typical conditions for aerospace aluminum alloys are around 480°C for 24 hours [13]. On slow cooling, S-phase (Al_2CuMg) particles will precipitate out first, peaking at around 410°C, for equilibrium conditions. At lower temperatures, M-phase ($Mg(Zn_2,AlCu)$) particles will start precipitating, reaching a maximum near 200°C, also for equilibrium conditions.

After the homogenization treatment, a significant amount of coarse intermetallic particles have been observed to remain at grain boundaries. Most un-dissolved particles that remain at the boundaries are the insoluble iron-rich Al_7Cu_2Fe particles; however, some of the particles are S-phase [13]. The homogenized structure also contains Al_3Zr dispersoids within the grains, primarily in regions near the center of cast dendrites, where local zirconium concentration is highest [13].

Following homogenization and slow cooling, a complex microstructure forms. Super-saturated aluminum quenched from the homogenizing temperature can precipitate fine solute particles upon preheating. However, for slow cooling, particles that nucleate during cooling will only coarsen during preheating.

Improved homogenization practices have been studied for aerospace aluminum. A two-stage homogenization treatment has been shown to improve dispersoid distribution in low-Zr regions and improve recrystallization resistance. This practice has reduced the recrystallized fraction in hot rolled and solutionized AA 7050 from 30 to 1% [21]. Experiments with higher-temperature homogenization treatments have reduced Zr concentration gradients [15].

Prior to hot deformation, the homogenized ingot is heated to the working temperature to reduce flow stress during processing.

1.2.3.1 HOT ROLLING

Hot working processes like hot rolling serve as the first step to convert cast material into a wrought product. Stored energy accumulated during hot rolling provides the driving force for recrystallization [10]. Deformation in hot working is usually performed above $0.6T_m$.

Hot working processes require low energy to deform the metal and there is increased material flow without cracking compared to cold deformation [23]. In multi-stage hot deformation of metals like aluminum, significant dynamic recovery/softening can reduce flow stress as the metal from one pass to the next [24]. Hot working also helps decrease chemical inhomogeneities in the cast structure, reduce/eliminate porosity, and refine coarse cast grains into smaller, equiaxed grains [23]. These microstructural changes increase the metal's toughness and ductility compared

to the cast ingot. Rapidly deformed and cooled metal requires a higher deformation temperature for the same amount of deformation than a slowly deformed and cooled metal [23].

There are, however, disadvantages to hot working. The elevated temperatures lead to surface reactions with the surrounding atmosphere. When exposed to air, the metal forms an oxide layer, which can potentially lead to considerable loss of metal. Additionally, oxide can be rolled into the surface making good surface finish difficult to achieve [23]. Hot-worked metals have higher dimensional tolerances than their cold-worked counterparts [23]. Reactive metals like titanium must be hot worked in an inert atmosphere or protected from air with a barrier. Significant surface finishing of hot-worked reactive metals is often required [23].

The "upper limit" for hot working is the temperature at which melting or excessive oxidation occurs. Working above this temperature allows for the possibility of lower-melting-point metals to melt and segregate or form a grain-boundary film. Very little of this liquid film is needed to lead to burning or hot shortness—the metal breaks apart during deformation due to sliding at the grain boundaries [23].

Most hot working operations are done in a number of passes with a deformation temperature well above the minimum working temperature to take advantage of lower flow stress. Higher temperatures allow for more grain growth. To reduce the grain size, the temperature is commonly lowered for the final pass such that grain growth during cooling will be minimized. The final pass typically has a larger deformation to decrease recrystallized grain size [23].

1.2.3.2 HOT ROLLED STRUCTURE

An additional complexity for hot-worked metal is a non-uniform structure that must be controlled as much as possible for large final products. The structure and properties of hot-worked metals are not as uniform as cold-worked and annealed metals throughout the thickness [16]. Hot rolling produces a complex structure with a number of interacting factors that determine the properties of the final product. Solutes are redistributed to the regions around the t/4 (quarter thickness) position, leaving the mid-plane (t/2) solute depleted. The gradient in quench rate contributes to the large variation in structure and composition throughout the thickness of hot-rolled plates [16]. During cooling, the interior regions of the work piece will remain at elevated temperatures longer than regions near the surface. Longer times at high temperatures allow for more grain growth and, in addition to lower deformation, lead to a coarser grain structure in the interior than at the surface [10, 16, 23]. Higher deformation in the surface region of the work piece will lead to a finer recrystallized grain structure in this region compared to the interior [10]. Slow cooling also leads to the heterogeneous nucleation and growth of large precipitates.

Local strain varies throughout the plate thickness. Shearing and high local strains at the surface compress and elongate grains, while deformation at the t/2 position is largely plane strain compression [8, 10]. The variation in stresses and strains throughout the structure gives a changing grain shape, dispersoid-free width, and stored energy through the plate. The stored energy accumulated is largely dependent on subgrain size and misorientation [10]. Stored energy is at a maximum near the plate surface, decreasing with depth up to 3t/8 beyond which it remains constant [10].

Crystallographic texture variation combined with the above factors produces a complex hot-rolled structure [8, 9, 16]. All of these parameters interact and influence one another, making it

difficult to isolate and control each factor without interfering with others. Hot rolling parameters must be optimized to produce the desired final microstructure and properties [5].

1.2.4 SOLUTIONIZING

Solutionizing is an annealing process that consists of heating the material to a high temperature (just below the eutectic temperature) long enough to allow other phases to go into solution. The metal is then quenched to room temperature, keeping the second phase in solution [20, 23]. Solution treatment of 7xxx series aluminum alloys must be at high temperatures to dissolve coarse second-phase particles. However, solutionizing at high temperatures promotes recrystallization [7]. Most, if not all, of recrystallization occurs during solution treatment of a metal [10].

If the solutionizing temperature exceeds the eutectic temperature, local melting will occur. Melting will expand the metal lattice due to solid-liquid volume expansion. Subsequent cooling leaves voids due to liquid-solid contraction. This is called “burning” [20]. If the cooling from the solutionizing temperature is too slow, solute elements are allowed time to diffuse and will form coarse precipitates on grain boundaries, depleting regions near the boundaries of solute atoms. This results in precipitation-free zones [20].

Following solution treatment and quenching, regions of recrystallized grains will be present. A fine dispersoid structure present prior to high temperature deformation can significantly suppress recrystallization in 7xxx series alloys [13]. Minimizing recrystallization in the final structure provides a balance of higher strength and toughness compared to a recrystallized structure [13].

1.2.5 AGING

An alloy with solute elements in solid solution can be aged, or age hardened, by heating the metal to a relatively low temperature that allows for diffusion and precipitation of the solute elements into particles. However, the aging temperature is too low to allow for significant dislocation movement, i.e. recovery and recrystallization. For an alloy to be capable of age hardening, the second phase must have decreasing solubility in the metal matrix with decreasing temperature. There is usually coherency between the matrix and particles [23]. Generally, lower precipitation temperatures for the solute is accompanied by higher hardness and yield strength; however, longer aging times are required at low temperatures. If the metal is aged too long, it becomes overaged and softening occurs—at some point, the material will become softer than the as-quenched metal where solution hardening is present. Solute concentration in the matrix decreases with increasing precipitation, decreasing solution hardening. This decrease in hardness is initially compensated by the increase in precipitation hardening until the particles become too large and too few, after which precipitation hardening decreases, as well [23].

1.3 ANNEALING

There are multiple stages of annealing that take place when deformed metals are heated. Initially, at lower temperatures, point defects will anneal out of the structure, generally with minimal effects on mechanical properties. Recovery is the next stage of annealing during which dislocations rearrange and annihilate. Following recovery, the metal will undergo recrystallization if there is sufficient stored energy to drive nucleation and growth of recrystallized grains. The last stage of annealing is grain growth whereby some recrystallized grains will grow, driven by free energy reduction from decreasing grain boundary area. During grain growth, larger grains generally grow at the expense of smaller grains. Recovery and grain growth processes are

reasonably homogeneous throughout the microstructure whereas recrystallization is heterogeneous [12].

The driving force for annealing processes is the stored energy in a deformed crystalline structure. Most of the energy used to deform the material is given off in heat with only about 1% remaining as stored energy in the structure [12]. The small fraction of energy that is stored is in defects—0-dimensional point defects and 1-dimensional dislocations. However, due to the high mobility of point defects, very little stored energy is contributed by them except at very low temperatures. There is also energy input in the form of increased boundary area—2-dimensional defects, however dislocation density and spatial distribution are the primary driving force of the recovery and recrystallization annealing processes [12].

1.3.1 RECOVERY

The process of recovery is one by which the properties of a deformed crystalline metal are partially restored. Recovery generally consists of several stages. Dislocations will initially rearrange by glide, climb, and cross-slip into dislocation tangles. The dislocation tangles will then rearrange into cell walls, forming a cell structure. Eventually subgrains will form and grow. This process leaves the metal in a metastable state where there are still dislocations present, but in a lower energy configuration due to dislocation rearrangement and annihilation [12].

Metal alloys with higher stacking fault energy (like aluminum) will typically form a cell structure that will rearrange into a subgrain structure upon further annealing. Dislocations annihilate and rearrange into low-angle, tilt boundaries that serve as subgrain walls [12]. Alloys with high stacking fault energy, low solute concentration, and high strains and deformation temperatures promote dynamic recovery—recovery that occurs during deformation. Dynamically

recovered metals form subgrains following deformation and further annealing will only coarsen the subgrain structure [3, 12].

Recovery can be inhibited by dispersed fine particles that interfere with dislocation movement and annihilation, possibly preventing low-angle boundary and subgrain formation, stabilizing a partially recovered structure. This can have an effect on recrystallization as it prevents subgrains from growing and developing sufficient misorientation to possibly serve as a nucleus for recrystallization [12].

1.3.2.1 RECRYSTALLIZATION

Recrystallization is the process whereby new grains with no strain or subgrain structure nucleate from a deformed structure and subsequently grow [12, 17, 25]. Recrystallization generally degrades mechanical and metallurgical properties of a metal and must be controlled in commercial processes [2, 7, 13]. The driving force for recrystallization is the reduction in free energy stored in a deformed structure [10, 12, 19]. Recrystallization and recovery are competing processes. Both are driven by stored energy—no more recovery can occur in a fully recrystallized structure. Conversely, as a structure recovers, the driving force for recrystallization decreases [6, 12].

Due to the inhomogeneous structure of hot-rolled plates, recrystallization can vary significantly throughout the thickness due to changes in stored energy and quantity, size, and spatial distribution of intermetallics and dispersoids. Texture and solute element concentration are also important factors influencing recrystallization [10, 19].

1.3.2.2 RECRYSTALLIZATION KINETICS

Stored energy is the driving force for metal recrystallization [6, 10, 12, 19]. For recrystallization to occur there must be sufficient stored energy to produce a nucleus that will be able to grow into a stable recrystallized grain [12]. Recrystallization requires a minimum deformation (between 1 and 5% strain) to occur. With higher deformation, more energy is stored in the structure and the recrystallization temperature is decreased [12, 23].

Recrystallization rate is primarily controlled by the amount of strain introduced into the metal and increases with increasing strain [12]. The type of deformation can also have an effect on the rate of recrystallization—straight rolling has been found to produce more rapid recrystallization compared to cross rolling, for example [12]. The rate of recrystallization in polycrystals may also depend on starting and deformation textures. Initial grain size also affects recrystallization rate. In general, fine-grained materials recrystallize more rapidly due to higher grain boundary area and increasing stored energy with decreasing grain size for materials with strains under 0.5 [12].

Recrystallization kinetics and final recrystallized grain size are particularly dependent on the size and spacing of second-phase particles. Particles in aluminum larger than one micron accelerate recrystallization when widely spaced [12].

Rapid heating to the annealing temperature may reduce the amount of recovery that can occur prior to recrystallization. This leaves more stored energy in the structure and increases recrystallization and promotes a finer recrystallized grain size [12]. In general, metal deformed at high temperatures and low strain rates will store less energy and recrystallize less than for a similar strain at a lower temperature, or higher strain rate [12].

1.3.2.3 PARTICLE STIMULATED NUCLEATION

Recrystallization in AA 7050 has been observed to occur by particle stimulated nucleation—nucleation at or near particles [2, 10]. Particle stimulated nucleation is a mechanism for recrystallization in both hot and cold deformation; however, it is much more prevalent in cold-deformed materials due to reduced static and dynamic recovery [26].

Recrystallized grains are often associated with large intermetallic particles along grain boundaries [10]. New nuclei are most likely to form at locations with high stored energy. Second-phase particles can disrupt material flow during deformation, increasing local dislocation density, orientation gradient and stored energy [2, 26]. Particles that deform with the matrix have weakened slip planes and further deformation will tend to concentrate the dislocations into slip bands. Particles that do not deform, however, will develop a strain incompatibility and compensate by forming geometrically necessary dislocations, increasing the local stored energy near the particles, providing potential locations for recrystallization [2, 12]. This is the basis for particle stimulated nucleation whereby new nuclei form in high-energy deformation zones surrounding sufficiently large particles [2, 12].

In rolled aluminum structures, recrystallization takes place by particle stimulated nucleation at an existing subgrain within the deformed zone surrounding a particle, but not necessarily at the particle surface. Rapid migration of the sub-boundary is the mechanism for nucleation [12].

Particle stimulated nucleation is known to have a critical size limit for particles to serve as nucleation sites. This size depends on deformation conditions (which vary through the structure of a thick rolled plate). Particles below the critical size will not nucleate recrystallized grains [10].

Critical size for particle stimulated nucleation decreases with increasing strain (stored energy) [12]. As the temperature of deformation increases, particle stimulated nucleation becomes a less viable mechanism for recrystallization. Dislocations may be able to interact with particles at high temperatures without forming deformation zones and stored energy is reduced. Particle stimulated nucleation will not occur if deformation has occurred above a critical temperature or below a critical strain rate [12].

Particles retained during rolling are generally large enough to serve as sites of particle stimulated nucleation for recrystallization [23]. It has been observed that large particles are found almost exclusively around the t/2 position of rolled plates—particles near the plate surface tend to be broken apart during rolling [10]. In a study by Robson and Pragnell in 2002, particles as large as 12-20 microns were observed at t/2 in hot-rolled 7050 with no particles exceeding 8 microns found at the surface [10]. Recrystallized fraction in hot-rolled AA 7050 were found to be greatest at the surface and t/2 position and least near t/4—fractions at the surface and t/2 exceed three times those at t/4 [10].

1.3.2.4 DYNAMIC AND STATIC RECRYSTALLIZATION

Recrystallization can occur statically or dynamically—subsequent to, or during high-temperature deformation. During thermomechanical processing, like hot rolling, recrystallization can occur between rolling passes or during the rolling reductions [2, 12]. Similarly, the annealing process of recovery can either be static or dynamic.

Metals with lower stacking fault energy like copper, nickel, and γ-iron have slow recovery processes and recrystallization can occur dynamically for a critical deformation condition [12].

Dynamic recrystallization forms at high-angle boundaries, original boundaries, dynamically recrystallized grain boundaries, or those associated with deformation bands [12].

As previously discussed, recovery and recrystallization processes compete for stored energy—prevalence of one will inhibit the other. Metals like aluminum, with high stacking fault energy, allow for easy dislocation climb and cross-slip. Consequently, dynamic recovery occurs quickly at elevated temperatures. The dynamic recovery in aluminum is typically so extensive that typically no dynamic recrystallization can occur [12].

There is little evidence to suggest that particle stimulated nucleation is a mechanism for *dynamic* recrystallization in aluminum alloys [12]. Particle stimulated nucleation would only be possible for deformation conditions by which dislocations accumulate at particles during deformation—requiring large particles and high strain rates at low deformation temperatures [12].

1.3.2.5 RECRYSTALLIZATION INHIBITORS

Transition elements like chromium, manganese, and zirconium are added to heat-treatable wrought alloys to form dispersoids, which control grain structure [6]. Dispersoid particles and solute elements are recognized, in general, as inhibitors to recrystallization. Al_3Zr dispersoids are of particular importance in 7xxx aluminum alloys, as they appear to inhibit recrystallization under the proper conditions [2, 6, 13-15].

Adding even small concentrations of Zr can control the grain structure of hot-worked, wrought aluminum alloys by controlling recrystallization [14, 15, 27]. Due to low solubility in aluminum, Zr precipitates out of the metal matrix during homogenization as Ll_2 Al_3Zr. Particles of Al_3Zr pin grain and subgrain boundaries, making nucleation and grain growth more difficult [2, 10,

15]. The effectiveness of dispersoids as a recrystallization inhibitor depends on particle size, spacing, volume fraction, and distribution [12, 14, 15]. Particles—large particles, in particular—can increase the stored energy in a structure by increasing dislocation density during deformation and serve as nucleation sites, promoting recrystallization. However, closely spaced fine particles significantly pin grain boundaries, interfering with recrystallization [12, 14, 15, 27]. The metastable Al_3Zr dispersoid particles are particularly effective inhibitors due to their resistance to transformation and coarsening—other dispersoids are less resistant at high temperatures [6].

In commercially produced aluminum alloys, zirconium dispersoids are generally distributed unevenly throughout the structure. Segregation of these particles, particularly during casting, leaves low-dispersoid regions in the structure, significantly more prone to recrystallization [14, 15]. Zirconium concentrations are highest at the middle, or t/2, position in hot-rolled aluminum. Microsegregation during casting also produces local variations in zirconium concentration, producing inhomogeneous dispersoid precipitation during homogenization [10].

Solutes in metal generally inhibit recrystallization. Solute elements may affect both nucleation and growth of recrystallized grains, primarily by influencing grain boundary mobility [12]. Solutes also affect the precipitation and distribution of Zr dispersoids. Scandium in combination with zirconium can improve dispersoid homogeneity as well as density, however it is generally too expensive to be cost-effective on an industrial scale [15]. Solute elements like Cu, Mg, and Zn have been predicted in 7xxx AA to accelerate Al_3Zr dispersoid precipitation kinetics compared with those of a binary Al-Zr system, with Mg predicted to have the strongest influence on accelerated precipitation [14]. Variation in solute elements and concentration throughout ingot and deformed ingot structure contribute to the complex recrystallization behavior of these materials.

Despite the t/2 position having low deformation and the highest concentration of Zr in rolled aluminum, recrystallization fractions are highest here (as well as the surface). This is possibly due to low-Zr regions near grain boundaries resulting from microsegregation forming fewer Al_3Zr dispersoids, leaving these areas more susceptible to recrystallization [10].

1.3.2.6 GRAIN GROWTH

Recrystallization is driven by the stored energy of deformation, but even following recrystallization, the metal structure is not yet stable. There is still energy stored in the boundaries between grains. Driven by the reduction in grain boundary area and the subsequent decrease in stored energy, grains will grow (when at sufficiently high temperature) [6, 12].

Though it often is, grain growth is not always preceded by recrystallization. There are two types of grain growth—normal and abnormal. During normal growth, microstructural changes are uniform and grain size and shapes fall within a limited range. During abnormal growth, few grains grow at the expense of smaller grains, giving a bimodal size distribution [12].

Grain growth is affected by a number of factors. The driving force for grain growth is around two orders of magnitude smaller than that of recrystallization [12]. Grain boundary mobility is temperature sensitive and most significant grain growth occurs at high temperature [12]. As previously discussed, grain boundary movement is impeded by solutes and particles. Grain growth is inhibited by fine particle dispersions and grains will stop growing when the pinning force is equal to the driving force for growth [12]. For thin materials, growth rate is reduced when the diameter of grains exceeds material thickness due to reduction in grain curvature in one direction.

Highly textured materials with a high number of low-angle grain boundaries have less stored energy to drive grain growth [12].

General effects of grain size on material properties are well understood. For relatively low temperature applications, strength and ductility are enhanced by a fine microstructure. For higher temperature applications, due to deformation by grain boundary sliding, a larger grain size is desired to improve creep resistance [12].

1.3.2.7 RECRYSTALLIZATION TEXTURES

Any recrystallization following deformation will have preferential nucleation associated with the certain features in structure. Preferential nucleation and growth of recrystallized grains will form a preferred recrystallization texture, different than the deformation texture it developed from [12].

Recrystallization by particle stimulated nucleation is not necessarily random relative to the orientation of the particles. However, unless the particles are specifically oriented, the recrystallized texture is expected to have a random texture relative to the deformed structure and grains recrystallized by other mechanisms [2]. This is particularly true for highly-rolled material containing large particles. Recrystallization textures for heavily-deformed alloys containing large fractions of particles are, in general, weak or randomly oriented [12].

1.4 DEFORMATION TEXTURES

In the process of polycrystalline metal deformation, preferred orientations can develop, forming a deformation texture. Crystallographic texture is determined by the deformation process and thermomechanical history of a structure [6]. Changes in orientation resulting from deformation

are due to easier deformation on favorably oriented slip systems [12]. Cubic metals deform primarily by slip and twinning. Face centered cubic structures (like aluminum) have relatively basic slip that predominantly occurs on the densely packed planes and directions: Miller indices {111}, <110>. Crystallographic texture is generally characterized by a continuous three-dimensional function that describes the distribution of crystallite orientation in a structure [28]. Deformation textures in a material depend strongly on the initial texture [28].

1.5 PLANE STRAIN TESTING

Plane strain testing is a commonly accepted method of simulating deformation conditions in ductile metals at room and elevated temperatures [29]. Strain distribution in plane strain compression testing is generally non-uniform. However, at the center of the deformed plane strain specimen, local strain changes less rapidly with position, making this the preferable location for metallographic analysis. Even minor offsets of the deformation surfaces in an experiment can lead to asymmetric material flow. Asymmetric flow is exaggerated with increasing deformation and results in a skewed “dog bone” shape of the deformed specimen. However, studies have revealed no significant influence of symmetric versus asymmetric material flow on the mid-plane texture evolution [29].

CHAPTER TWO

RESEARCH DESIGN AND METHODOLOGY

2.1 UNIAXIAL DEFORMATION EXPERIMENTS

To investigate stored energy in an already-rolled AA 7050 plate, specimens of that alloy were deformed and the recrystallized fraction was measured relative to strain, strain rate, and deformation temperature. Specimens were deformed in uniaxial compression to different strains at varying strain rates and deformation temperatures.

Cylindrical uniaxial deformation specimens were sectioned and machined from 5-inch rolled plate of AA 7050. The nominal composition of the 7050 was 5.7% Zn, 2% Cu, 1.9% Mg, 0.12% Zr (weight%), trace amounts of Fe, Si, Mn, Cr, and Ti with the remaining weight/volume fraction being aluminum. Initial specimen dimensions were 8mm (± 0.1mm) in diameter and 12mm long. Specimens were initially machined into 5-inch long, 8mm-diameter cylinders (cylinder axis aligned with the normal direction, ND, of the plate), denoted in series A-G. The 5-inch long specimens were then sectioned into 8 sequentially numbered cylinders, each 12mm tall. This study focused on the behavior of the rolled material at t/2. Specimens at the 4 and 5 position—closest to the t/2 position of the plate—were used for final deformation experiments. Other specimens were only used for test calibrations.

Deformations of 0.1 and 0.4 strain at rates of approximately 0.2, 0.7, 2.3, and 8.0 s^{-1} were performed. Deformations were carried out at 385, 425, and 465°C. These parameters cover the range of potential conditions present in common industrial hot rolling practices. Due to time and specimen constraints, every one of these deformation conditions could not be tested. For each total strain, a sequence of varying strain rates for the same deformation temperature and varying

deformation temperatures for the same strain rate were tested (see Table 2.1). Conditions were selected to provide the most insight into material behavior at deformation conditions best approximating those actually present during the hot rolling process of interest.

Table 2.1: Uniaxial test conditions. Conditions in gray were not performed. All strain rates are in units of s^{-1}.

		Total Strain							
		0.1 [mm/mm]				0.4 [mm/mm]			
Def. Temp.	385°C specimen	r=0.2	r=0.7 E4	r=2.3	r=8.0	r=0.2	r=0.7 E5	r=2.3	r=8.0
	425°C specimen	r=0.2 G4	r=0.7 B4	r=2.3 C4	r=8.0 D4	r=0.2 D5	r=0.7 B5	r=2.3 C5	r=8.0 G5
	465°C specimen	r=0.2	r=0.7 F4	r=2.3	r=8.0	r=0.2	r=0.7 F5	r=2.3	r=8.0

The experiments were performed at the University of British Colombia in Vancouver, BC on a Gleeble 3500 machine. The Gleeble testing machine allows for precise temperature and deformation control and has a helium gas quench. It is also capable of high strain rates. Specimens were heated to temperature using self resistance heating at a rate of approximately 5°C/s, deformed at the specified experimental conditions, and quenched.

Naming convention for the uniaxial specimens was *Gleeble_385_01_80 T6*. *Gleeble* denotes the experiment was deformed under uniaxial compression on the Gleeble 3500. The *385* indicates a deformation temperature of 385°C. The strain, 0.1 mm/mm, is noted by *01*. Similarly, the strain rate of $8.0s^{-1}$ noted by *80*, note: there is no decimal point used. A strain rate of 0.2 would be represented by *02*. *T6* indicates the specimen was T6 peak aged after deformation.

2.2 PLANE STRAIN EXPERIMENTS

Plane strain testing is a commonly accepted experiment for simulating deformation conditions at the mid-plane of rolled material [29]. Specimens were deformed in plane strain

compression at conditions similar to those present in common industrial hot rolling practices. The nominal composition of the 7050 used for plane strain testing was 6.21% Zn, 2.06% Cu, 2.08% Mg, 0.101% Zr (weight%), trace amounts of Fe, Si, Mn, and Cr with the remaining weight/volume fraction being aluminum.

Rectangular plane strain specimens were machined from AA 7050 the t/2 (mid-plane) position of a homogenized ingot slice. This study was concerned with the deformation conditions at the center of a homogenized ingot during hot rolling. These conditions approximated those at the center of the plane strain specimen. Initial specimen dimensions were 8 by 15 by 25mm (± 0.1mm). The nominal composition of the alloy was similar to that of the metal used in the uniaxial experiment, but with 0.08% Zr.

Plane strain rams were designed to operate using the Materials Testing System (MTS), as well as to work within the dimensions of the external clamshell furnace used to heat the system. The rams are identical; each has a deformation surface 5mm wide (± 0.1mm) with a 25 degree taper off the vertical axis and is at the end of a 25.4-mm (1-inch) diameter H-13 tool steel rod, designed to fit inside the furnace openings (see Figures 2.2 a, b). The steel was heat-treated to a hardness of RC 50. Ram design was patterned around existing plane strain compression system designs.

Deformation conditions of the experiment consisted of strain rates of approximately 0.2, 0.7, and 2.3 s^{-1} at temperatures of 385, 425, and 465°C (± 5°C—the furnace used lacks the precise temperature control of the Gleeble system). Total deformation of the specimens simulated rolling reductions from an initial 'scalped' plate thickness of 18.8 inches to 16, 4, and 2 inches (see Table 2.2). Actual specimen deformations were from 8.00mm to 6.81, 1.70, and 0.85mm—or total strains

of 0.15, 0.79, and 0.89, respectively. The 8 to 6.81-mm deformations were carried out in 9 steps simulating individual rolling passes. There was a 30-second pause between each step. The 6.81 to 1.70-mm deformations were performed in 8 steps with 15-second pauses. The 1.70 to 0.85-mm deformations were performed in 4 steps with 10-second pauses.

Table 2.2: Plane strain test conditions. All strain rates (r) are in units of s^{-1}.

		Total Strain								
		0.15 [mm/mm]			0.79 [mm/mm]			0.89 [mm/mm]		
Def. Temp	385°C	r=0.2	r=0.7	r=2.3	r=0.2	r=0.7	r=2.3	r=0.2	r=0.7	r=2.3
	425°C	r=0.2	r=0.7	r=2.3	r=0.2	r=0.7	r=2.3	r=0.2	r=0.7	r=2.3
	465°C	r=0.2	r=0.7	r=2.3	r=0.2	r=0.7	r=2.3	r=0.2	r=0.7	r=2.3

A Materials Testing System machine operated by TestWare SX/ TestStar was used to perform the experiment. The upper cross-head on the MTS can be moved to any desired position prior to running a test program, but is locked in place during testing. The lower press can be manually moved or programmed to move to specific positions at a desired rate. There are hydraulic collets on upper and lower portions of the machine that grip the plane strain rams.

A collar was made to constrain lateral movement of the ram surfaces during testing (see Figure 2.2 c). The collar fit around the ends of both rams, but did not restrict axial movement. It was held in place with a set-screw that was secured to the top ram. Even with proper ram alignment prior to testing, without the constraint of the collar, the inhomogeneous nature of ingot deformation resolved sufficient stresses to offset the ram surfaces and skew the deformation, taking the specimens out of plane strain.

Prior to deformation, the specimen and rams were heated using an external electric clamshell furnace. Due to the length of the rams, thermal conduction into the surrounding air prevented any significant heat transfer into the MTS machine. Two external thermocouples were

attached to the collar with safety wire to system, near the specimens, to ensure consistent, accurate temperature measurements were taken.

Plane strain ram positions and velocity were calculated to match the various deformation conditions and programmed into TestWare SX/ TestStar. The system uses an absolute position system. A “zero position” point was chosen and calculated into the position data to prevent variation in the deformation due to varying initial ram position.

The lower plane strain ram was set to the zero position prior to each test. The specimen was then coated with a copper-based high-temperature lubricant and placed perpendicular to the long axis of the ram deformation surface and at the approximate center of the ram. The upper ram was set near the top of the specimen, but not contacting it, and the furnace closed and set to the appropriate temperature. If the top ram was brought into contact with the specimen, upon heating, thermal expansion of the system would generate in excess of 3300 pounds compressive force and would deform the specimen prior to the test and result in excessive deformation. Once the system was at the desired temperature for deformation, the top ram was carefully brought into contact with the specimen and locked in place. The experiment program then ran and the specimen was quenched in a room temperature water bath within approximately 5 seconds of the completion of the experiment.

Initially, after each deformation step simulating one rolling pass, the ram was kept in place until the next deformation. However, this resulted in force being constantly applied to specimen between passes (up to 1000 pounds) and excessively deformed the specimen in addition to altering the deformation conditions. To prevent this from occurring, the ram was programmed to be stepped

back 0.1mm following each pass. This reduced force applied between passes to between 0 and 50 pounds.

Due to the long pauses between deformations, no numerical strain/ strain rate data was collected. Data collection files were limited in the number of data points that could be collected. At collection frequencies low enough to cover the duration of the experiments, the deformations occurred too quickly to be measured.

Naming convention for the plane strain specimen was *Zr10_425_20-2_r02_1min*. *Zr10* indicates the composition of the alloy used—*Zr10* for 0.10% Zr. Similarly, *Zr12* was used for 0.12% Zr (the same alloy used in uniaxial compression tests). Note: all final results are from the 0.10%-Zr composition. The *425* indicates the deformation temperature of 425°C. The strain is indicated by *20-2*, for simulating the approximate initial height of 20" to the final deformed height of 2". This is actually 18.8-2", or a strain of 0.89. Similarly, *20-16* and *20-4* were used for strains of 0.15 and 0.79, respectively. The strain rate of $0.2s^{-1}$ noted by *r02*. The *1min* indicates the specimen deformed under the previous conditions was annealed for 1 minute at 465°C.

2.3 HEAT TREATMENT

All uniaxial specimens were heat-treated to the T6 aged condition—annealed 1 hour at 465°C and quenched, followed by a 24-hour age at 121°C. A limited investigation of recrystallization in as-quenched specimens was yielding little results due to a relatively high concentration of Zr in the 5" plate alloy, which inhibited recrystallization. All uniaxial specimens were peak aged to fully recrystallize the deformed structure. Note: due to the limited recrystallization results, no data for quantitative comparison between the as-quenched and T6 conditions was taken.

After being quenched, the plane strain specimens were annealed for various times to determine the stored energy in the structure by recrystallization analysis at various stages of deformation. Some specimens were sectioned in half, so that the ND-LT cross section (see Figure 2.3.1) could be analyzed, and heat-treated. Others were sectioned such that around the center of the deformed region, three approximately 1.5 by 5mm specimens were made from the region in plane strain and heat-treated (see Figure 2.3.2). Specimens were sectioned to allow for a maximum number of heat treatment conditions while minimizing the number of deformation experiments that needed to be carried out.

The specimens were annealed at 465°C for 30, 60, 600, 1200 seconds—some specimens were also analyzed in the as-quenched condition. All specimens were aged at 121°C for 24 hours to precipitate out elements in solution and allow the metal to be properly etched for optical microscopy analysis. At higher temperatures, dislocations can move and the structure can recrystallize—the amount of which depends on the stored energy of the structure—however, at lower, aging temperatures, there is only enough energy available to precipitate out supersaturated elements.

2.4 METALLOGRAPHY

Following heat treatment, the uniaxial specimens were sectioned at the mid-plane of the deformed cylinder and mounted in phenolic resin. Plane strain specimens were mounted in either epoxy or phenolic resin. The sectioned 1 by 5mm specimens were ground to the mid-plane so they could be analyzed in the L-LT section (see Figure 2.3.2). All specimens were then polished according to standard metallographic procedures. After being ground to 1200 grit (21 micron) grinding paper, the specimens were polished with 1-micron diamond paste, 0.05-micron alumina

solution, and 0.01-micron MgO powder. For optical recrystallization analysis, all specimens were etched in a 10% phosporic (H_3PO_4) acid solution at around 45°C for 15-17 minutes and then imaged on an optical microscope.

CHAPTER TWO FIGURES

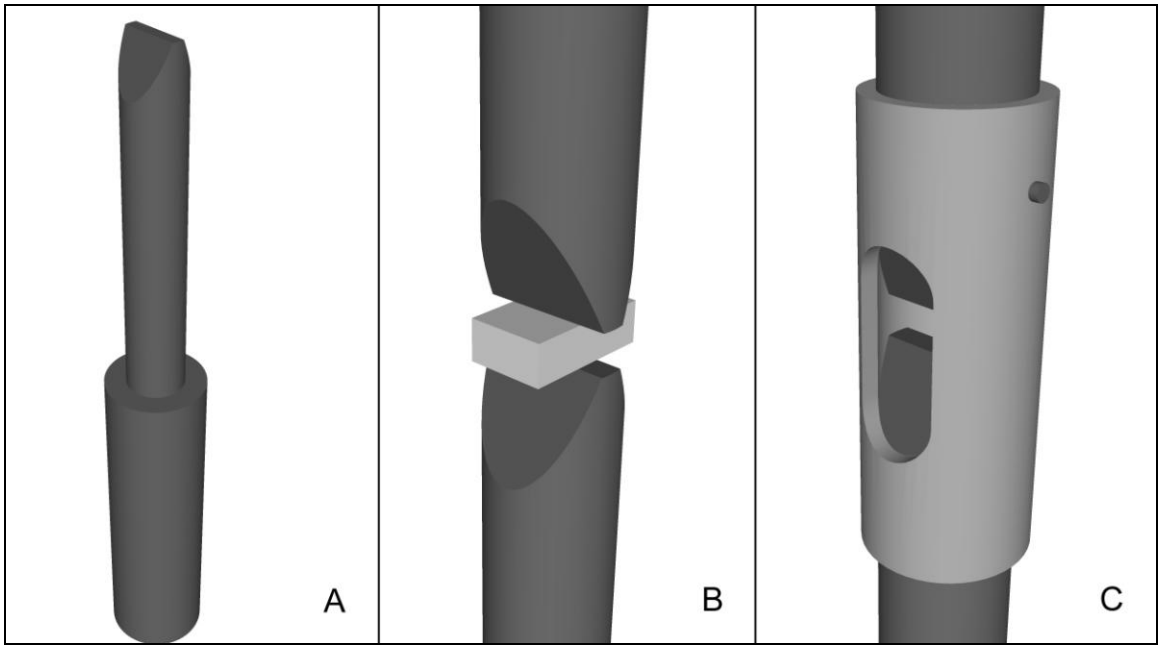

Figure 2.2: A) Plane strain ram. B) Close up view of the two rams in contact with an un-deformed specimen. C) Close up view of the two rams constrained by the collar.

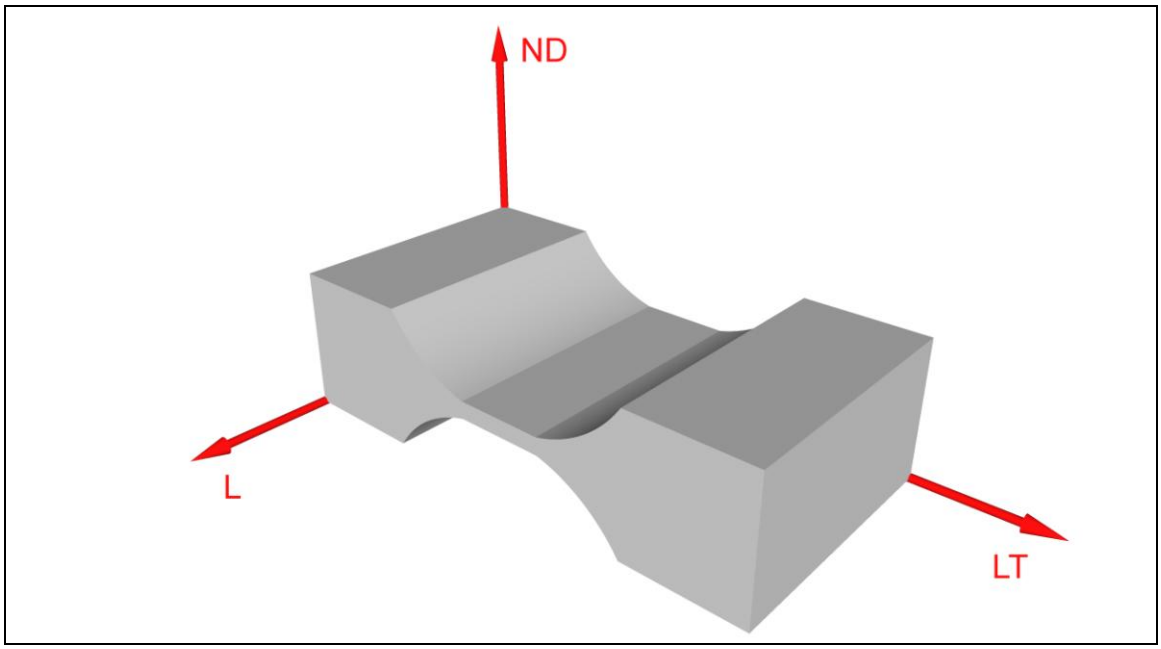

Figure 2.3.1: Coordinate axes for the plane strain specimen (shown deformed to 0.89 strain). ND – normal direction (initial height 8mm), LT – long, transverse direction (initial length approximately 25mm), L – long direction (initial width 15mm).

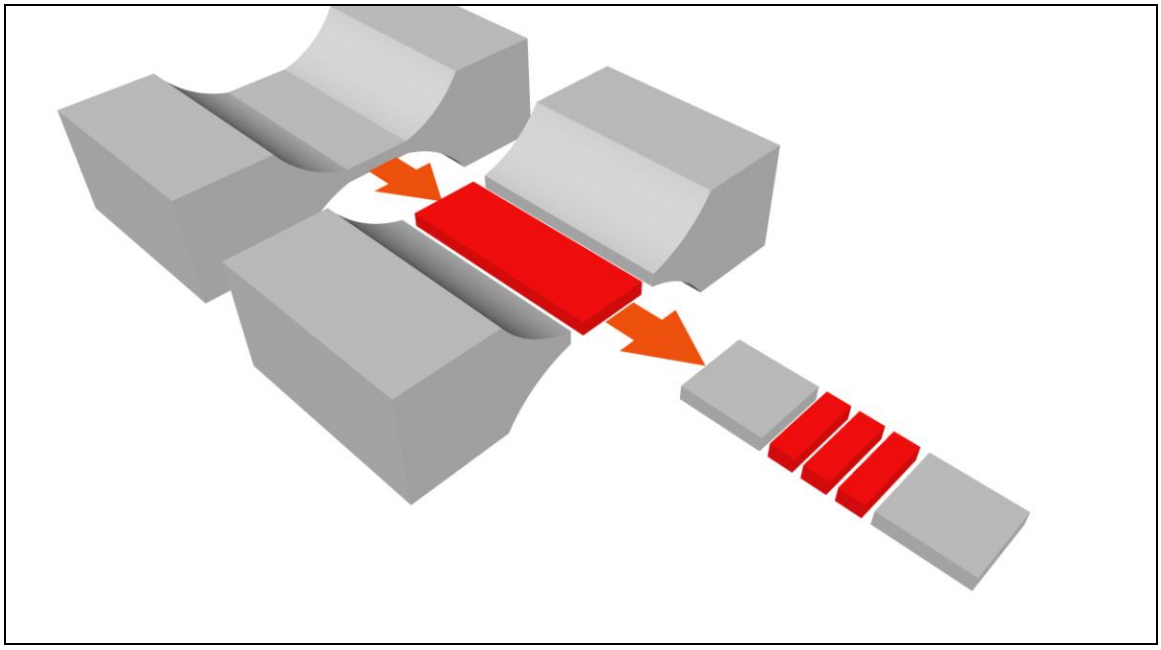

Figure 2.3.2: Deformed plane strain specimen sectioned for heat treatment. Ground to the mid-plane (in the ND) for analysis in the L-LT plane.

CHAPTER THREE

ANALYSIS

3.1 UNIAXIAL DEFORMATION ANALYSIS

For all uniaxial specimens, the region near the center of the deformed cylinder was imaged in nine sequential photographs in a three-by-three grid centered at the approximate center of the specimen. The images were taken at relatively low magnifications (between 20 and 30x) and the recrystallized fraction was measured using a point count method (summing the points of intersection on a grid that lie over a feature of interest and dividing that number by the total number of intersections). Recrystallized regions in the structure are identifiable in optical microscopy due to their structure. Recrystallized grains are newly nucleated grains with little to no deformation or subgrain structure and generally appear white. In contrast, material that is deformed or recovered appears darker [13]. Recrystallized grains that are over-etched do, however, appear darker, but they do not have apparent deformation or subgrain structure (see Figure 3.1.1). The average total area of analysis for each specimen was approximately 14 mm^2. The total number of points measured per specimen was 1170. There was no variation in the number of points analyzed from specimen to specimen. Any point entirely on a recrystallized grain was counted as 1 and any point on a boundary between a recrystallized and un-recrystallized grain was counted as ½ (see Figure 3.1.2 for an example image of the point count method).

3.2 UNIAXIAL DEFORMATION RESULTS

The recrystallized fraction of the 5-inch rolled plate, t/2 position AA 7050 deformed in uniaxial compression generally followed expected trends. The recrystallized fraction for each tested condition is detailed in Table 3.2.

Table 3.2: Uniaxial test recrystallization results. Conditions in gray were not performed. All strain rates (r) are in units of s^{-1}.

		Total Strain							
		0.1 [mm/mm]				0.4 [mm/mm]			
Def. Temp.	385°C *RX%*	r=0.2	r=0.7 *10.51%*	r=2.3	r=8.0	r=0.2	r=0.7 *12.61%*	r=2.3	r=8.0
	425°C *RX%*	r=0.2 *1.79%*	r=0.7 *7.39%*	r=2.3 *	r=8.0 *12.18%*	r=0.2 *9.32%*	r=0.7 *11.07%*	r=2.3 *14.06%*	r=8.0 *20.17%*
	465°C *RX%*	r=0.2	r=0.7 *5.85%*	r=2.3	r=8.0	r=0.2	r=0.7 *9.53%*	r=2.3	r=8.0

*** Specimen damaged during the annealing process. No data collected for this set of conditions.**

3.2.1 RECRYSTALLIZATION AND STRAIN

Recrystallization increases with increasing strain for all available data as seen in Table 3.2.1. This trend is also illustrated comparing the 0.1- and 0.4-strain Gleeble data series in Figure 3.2.1. Given current understanding of recrystallization as a function of deformation conditions, it would be reasonable to expect that the missing data point (425°C, 0.1 strain, and strain rate of 2.3 s^{-1}) would fall between 7.39 and 12.18% of the 0.7 and 8.0s^{-1} conditions, respectively. If this were the case, the trend present would be upheld. The recrystallized fraction for the uniaxial compression tests also increases with increasing strain rate for a given deformation (see Figure 3.2.1). This is consistent with the understanding that increasing deformation and deformation rate will put additional stored energy into a structure that serves as the driving force for recrystallization.

3.2.2 RECRYSTALLIZATION AND DEFORMATION TEMPERATURE

For both deformation levels, recrystallized fraction decreases with increasing deformation temperature (see Figure 3.2.2). Considerable dynamic recovery has been previously been observed in aluminum deformed in multiple steps at 400°C [24]. Due to extensive, favorable dynamic

recovery in aluminum alloys, stored energy is consumed in the recovery process and the driving force for subsequent recrystallization is reduced. As deformation temperature increases, recovery occurs more readily and further decreases the driving force for recrystallization.

3.3 PLANE STRAIN ANALYSIS

For all plane strain specimens, the entire (approximately 5mm-long) region of deformation was imaged in sequential photographs at relatively low magnifications (between 20 and 30x) and the recrystallized fraction was measured using a point count method. The average total area of analysis for each specimen was approximately 8.5 mm^2. The total number of points measured was approximately 720 with a standard deviation of around 220 due to variation in sectioned specimen size—there was one specimen significantly smaller than the rest and only 270 data points were able to be measured. The maximum points measured for a specimen was 1728. Any point entirely on a recrystallized grain was counted as 1 and any point on a boundary between a recrystallized and un-recrystallized grain was counted as ½ (see Figure 3.1.2).

3.4 PLANE STRAIN RESULTS

3.4.1 RECRYSTALLIZATION AND STRAIN

In general, recrystallization increases with increasing strain (see Figures 3.4.1a-c) in agreement with the results for the uniaxial compression tests. There are some exceptions: see the *Zr10_385_r07_20min* series in Figure 3.4.1a and the *Zr10_465_r02_20min* series in Figure 3.4.1c.

Precise quantitative recrystallization results (from one condition to the next) for the plane strain tests were more difficult to attain than for the uniaxial experiments. Due to smaller sectioned specimen size (see Figure 2.3.2), it was more difficult to get the specimen sectioned to the mid-plane (the region of most-ideal deformation for the experiments). The temperature of the plane

strain system was also less precise than for the Gleeble 3500 setup. Temperatures were ±5°C for the plane strain tests compared to variation within 0.1 to 0.2°C for the Gleeble tests. Temperature was measured externally from the plane strain deformation program and the setup did not allow for temperature data collection during the experiments. Quenching was done by hand, with the specimens cooled to room temperature within approximately 5 seconds. Specimens that exceeded this quench timeframe were not considered valid and the experiment was redone.

3.4.2 RECRYSTALLIZATION AND STRAIN RATE

Recrystallized fraction for the plane strain tests (following solution treatment) generally increases with increasing strain rate (see Figures 3.4.2.1a-c). There is an exception in the data (see the *Zr10_465_r07_20min* series in Figure 3.4.2.1c), however, it is likely due to the reasons discussed above, in the *3.2.1 Recrystallization and Strain*. From Figures 3.4.2.1a-c, it appears that for lower strain rates, the difference in recrystallized fractions between deformation temperature conditions generally decreases (particularly in Figure c). Conversely, higher strain rates tend to increase the difference between high- and low-deformation temperature recrystallization. This trend is also visible in Figure 3.4.2.2.

3.4.3 RECRYSTALLIZATION AND DEFORMATION TEMPERATURE

Similar to the uniaxial compression results, recrystallization for solution-treated specimens generally decreases with increasing deformation temperature (see Figures 3.4.3.1a and b and Figure 3.4.3.2; this trend is also illustrated by comparing Figure 3.4.1a to Figures b and c). Extensive recovery that becomes more prevalent with increasing temperature reduces the driving force for recrystallization, as discussed in *3.2.2 Recrystallization and Deformation Temperature*. An exception to this trend is visible in the 20-minute solution-treated specimens deformed at $0.2s^{-1}$ (see the *Zr10_20-2_r02* series in Figure 3.4.3.1b). The recrystallized fraction for this strain rate is

approximately constant around 12% at this strain rate for all deformation temperatures. This 12% recrystallized fraction is also present for a higher rate of $0.7s^{-1}$ at 425°C and for all strain rates at 465°C. As the deformation temperature increases, the driving force for recrystallization decreases, yet all conditions have a minimum amount of recrystallization. This suggests that for a structure hot-deformed to high strains (0.89 in this study) and sufficiently annealed, that there will be a minimum amount of recrystallization due to the input energy of deformation (regardless of other thermomechanical processing conditions).

It appears that as the deformation temperature increases the importance of strain rate relative to recrystallization decreases (see Figures 3.4.3.1a and b). It is possible that at higher deformation temperatures, the aluminum is able to dynamically recover rapidly enough to prevent increasing strain rates from storing significant additional energy to drive recrystallization.

3.4.4 RECRYSTALLIZATION AND ANNEALING TIME

The recrystallized fraction for as-quenched plane strain tests was zero for most experimental conditions. However, some recrystallization was detected for as-quenched, high strain, high strain rate conditions. For a strain rate of $2.3s^{-1}$ and strains of 0.79 and 0.89, there was 0.77 and 7.77% recrystallization, respectively (see Table 3.4.4).

It is possible that the relatively high strain rate combined with a high deformation and inter-pass holding (annealing) temperature that there is sufficient driving force to recover and recrystallize some parts of the structure. For the conditions of this experiment, there is no way to determine whether this recrystallization occurred during or after deformation. In previous studies on AA 7050 (deformed by uniaxial, hot deformation), *dynamic recovery* was the primary softening mechanism for experiments between 340 and 420°C. *Dynamic recrystallization* was the primary

Table 3.4.4: Plane strain test recrystallization [%] results. All strain rates (r) are in units of s^{-1}.

	Total Strain, Annealing Time								
	0.89 [mm/mm], as-quenched			0.79 [mm/mm], as-quenched			0.15 [mm/mm], as-quenched		
	r=02	r=07	r=23	r=02	r=07	r=23	r=02	r=07	r=23
385°C	0.00%	0.00%	0.00%	0.00%	0.00%	0.00%	0.00%	0.00%	0.00%
425°C	0.00%	0.00%	0.00%	0.00%	0.00%	0.00%	0.00%	0.00%	0.00%
465°C	0.00%	0.00%	7.77%	0.00%	0.00%	0.77%	0.00%	0.00%	0.00%
	0.89 [mm/mm], 30s								
	r=02	r=07	r=23						
385°C	5.48%	5.39%	12.83%						
425°C	1.39%	9.26%	6.15%						
465°C	0.86%	2.21%	5.11%						
	0.89 [mm/mm], 60s								
	r=02	r=07	r=23						
385°C	4.48%	19.93%	29.01%						
425°C	6.28%	14.15%	15.38%						
465°C	1.69%	*	15.10%						
	0.89 [mm/mm], 600s								
	r=02	r=07	r=23						
385°C	15.76%	20.73%	26.55%						
425°C	9.73%	11.52%	17.42%						
465°C	4.38%	7.76%	8.97%						
	0.89 [mm/mm], 1200s			0.79 [mm/mm]			0.15 [mm/mm]		
	r=02	r=07	r=23	r=02	r=07	r=23	r=02	r=07	r=23
385°C	12.01%	20.36%	27.64%	6.71%	24.66%	20.58%	6.08%	11.46%	14.69%
425°C	12.22%	12.14%	19.98%	4.65%	11.54%	14.74%	2.66%	8.33%	7.18%
465°C	11.88%	10.84%	11.32%	13.24%	9.49%	9.10%	2.46%	3.13%	4.31%

*** Specimen damaged during the annealing process. No data collected for this set of conditions.**

softening mechanism for alloy deformed at 460°C [1]. The results are consistent with respect to recovery dominating lower-deformation temperature softening processes. Recrystallization occurring for higher-deformation temperature was also confirmed, but it was not determined in this study whether or not the recrystallization was dynamic (pauses between deformations were between 10 and 15 seconds near these final deformation levels, times possibly long enough to partially recrystallize the structure). Regardless, these results indicate that AA 7050 deformed under these conditions in hot rolling will produce recrystallization at the t/2 position without any further heat treatment.

The recrystallized fraction of the deformed specimens is at or near the maximum value (for the range of annealing time data) within 60 seconds, as can be seen in Figures 3.4.4a-c. Recrystallization as a function of time has been observed in aluminum to have a sigmoidal form [2]. That is, the recrystallization will initially occur slowly, followed by a region of rapid transformation before slowing again and leveling off towards a maximum value. In this study, it appears that for the conditions present, recrystallization occurs rapidly before possibly leveling off without an initial slow period.

CHAPTER THREE FIGURES

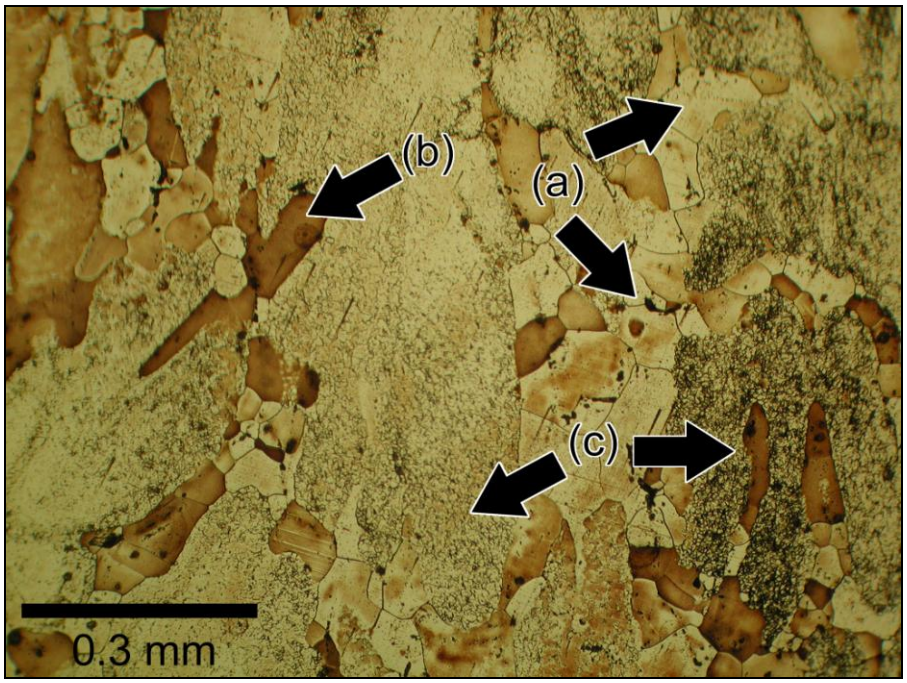

Figure 3.1.1: Identified features of recrystallized structure (specimen Zr10_385_20-2_r23_10min). Recrystallized grains (a), over-etched recrystallized grain (b), deformed matrix (c).

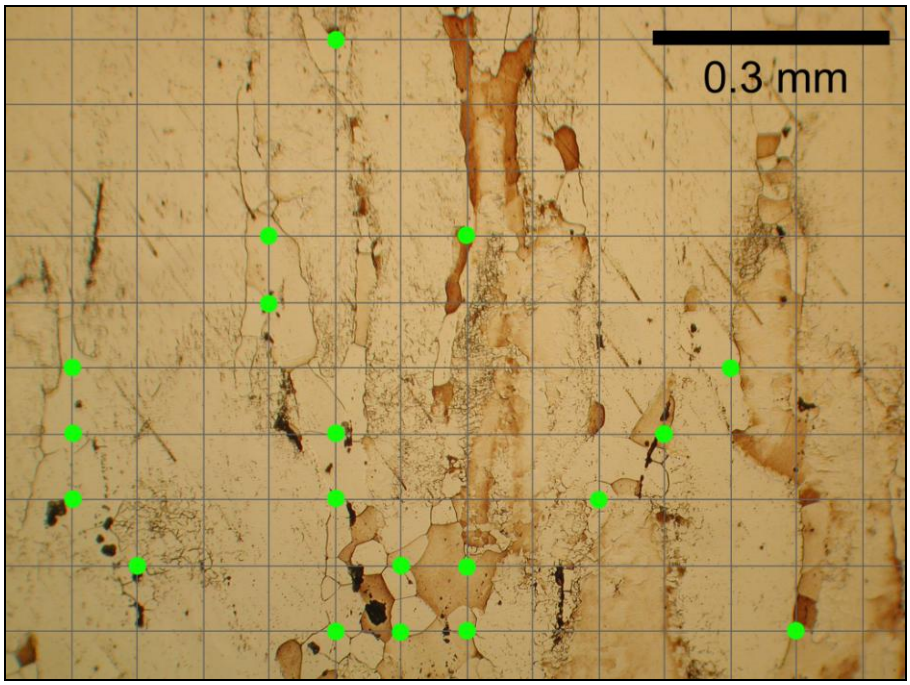

Figure 3.1.2: A typical image of recrystallization analysis of hot-deformed aluminum (specimen Gleeble_425_04_80). Point of intersections on recrystallized grains marked as green dots.

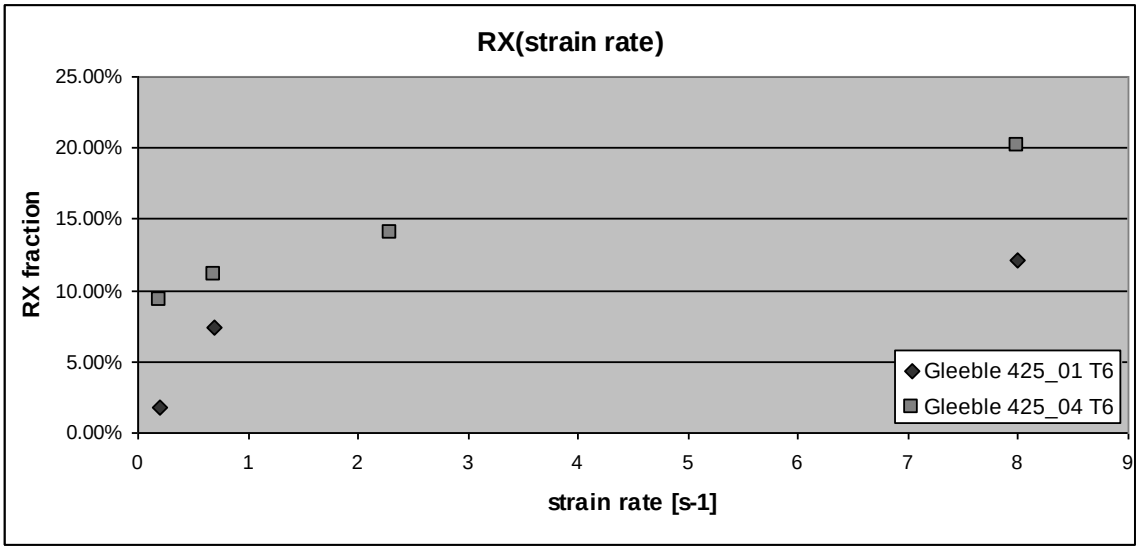

Figure 3.2.1: Recrystallization as a function of strain rate for the uniaxial compression tests. Note: the data point for *Gleeble 425_01_r23* is absent due to damage during the annealing process. No data was collected for this set of conditions. All specimens were T6, peak aged.

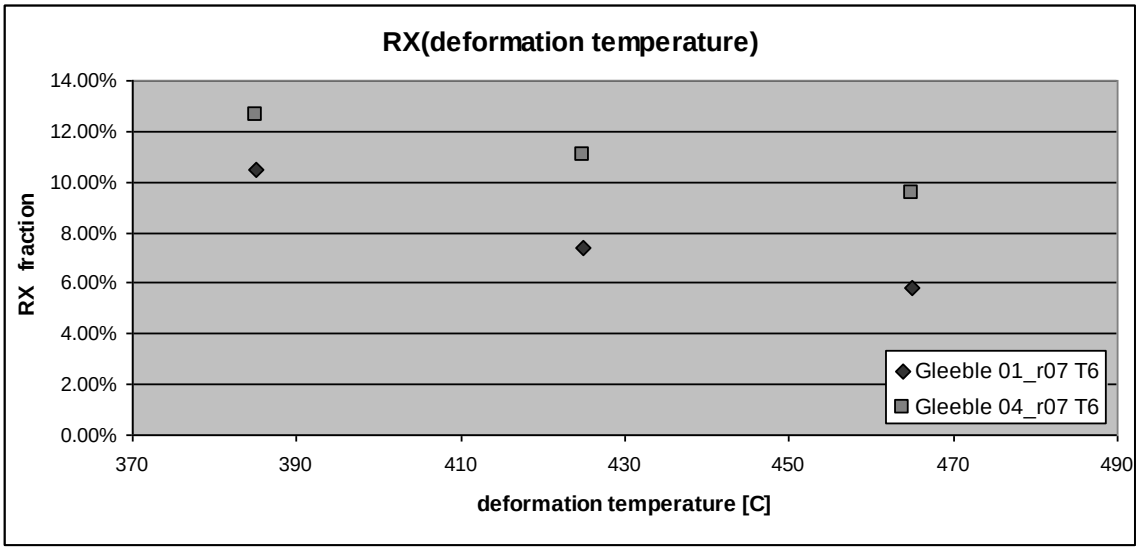

Figure 3.2.2: Recrystallization as a function of deformation temperature for the uniaxial compression tests. Note: all specimens were T6, peak aged.

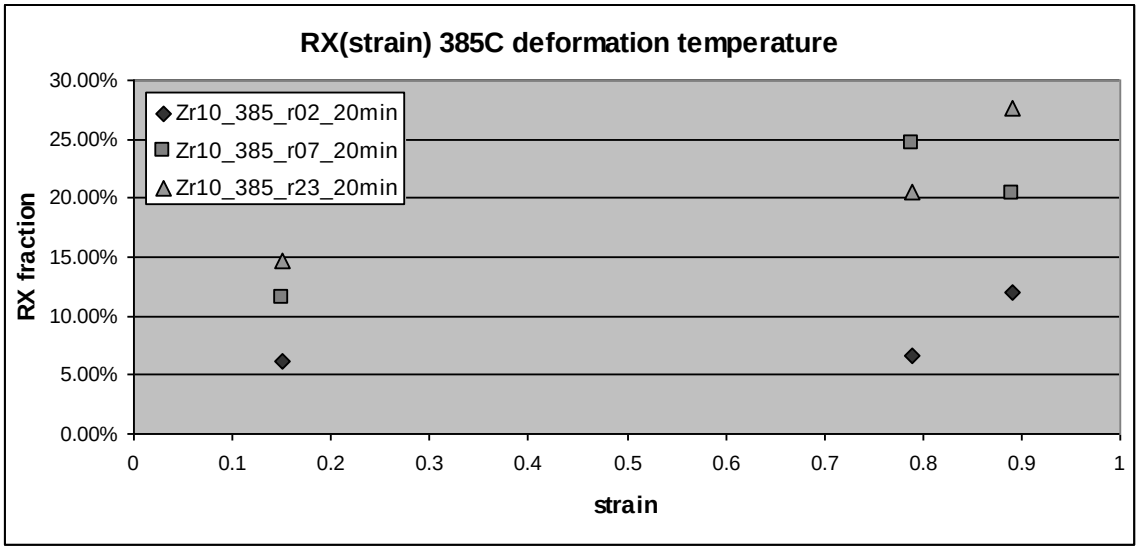

Figure 3.4.1a: Recrystallization as a function of strain for the plane strain compression tests (deformed at 385°C, annealed 20 minutes at 465°C).

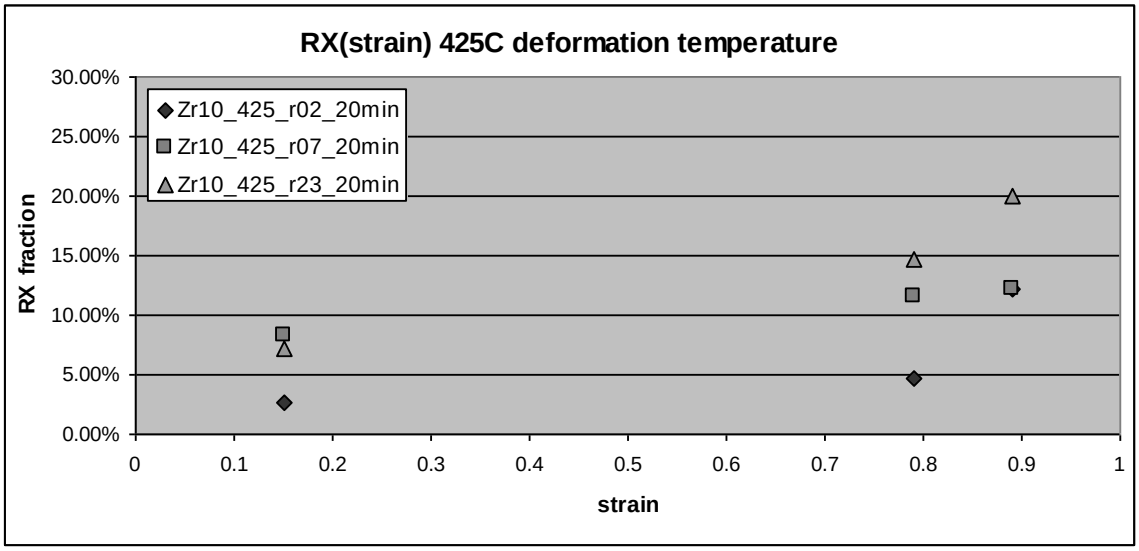

Figure 3.4.1b: Recrystallization as a function of strain for the plane strain compression tests (deformed at 425°C, annealed 20 minutes at 465°C). Note: for the 0.89-strain condition, the $0.2s^{-1}$- and $0.7s^{-1}$-strain rate conditions overlap around 12% recrystallization.

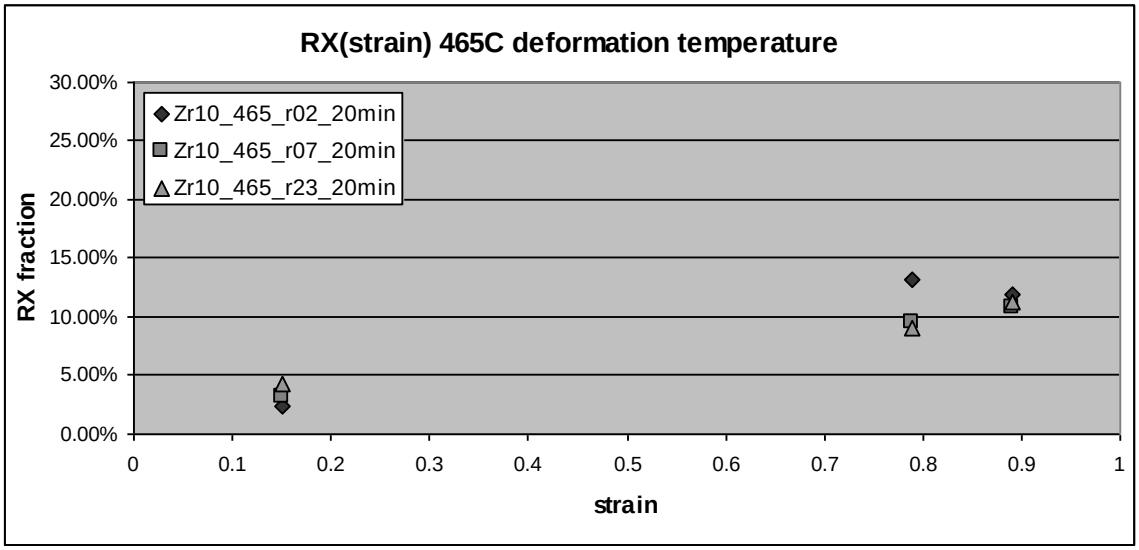

Figure 3.4.1c: Recrystallization as a function of strain for the plane strain compression tests (deformed at 465°C, annealed 20 minutes at 465°C). Note: all three data points for the 0.89-strain condition overlap around 11% recrystallization.

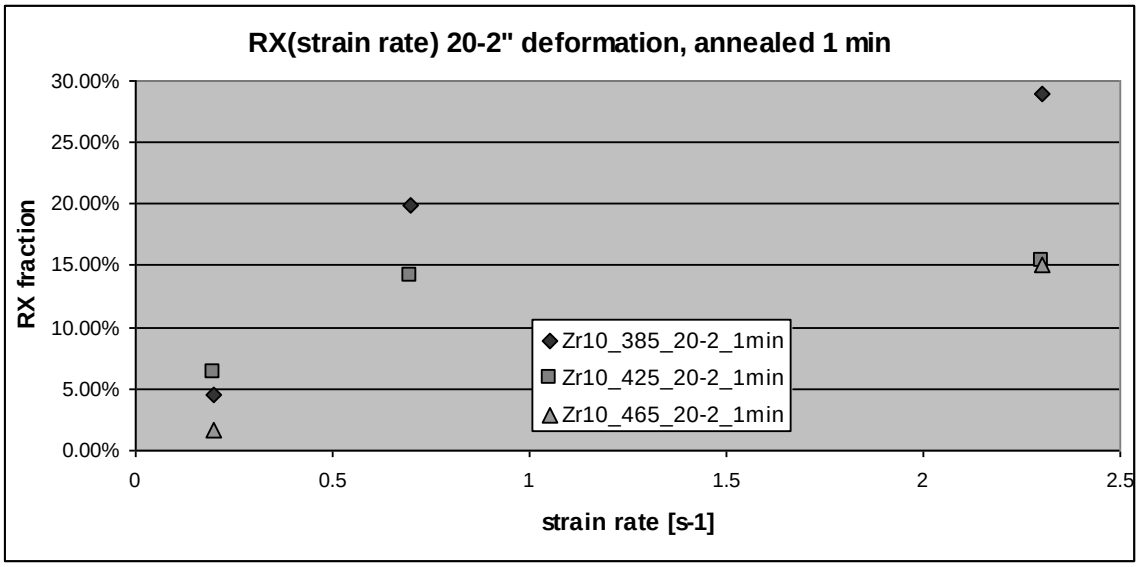

Figure 3.4.2.1a: Recrystallization as a function of strain rate for the plane strain compression tests (annealed at 465°C for 1 minute). Note: the data point for *Zr10_465_20-2_r07_1min* is absent due to damage during the annealing process. No data was collected for this set of conditions.

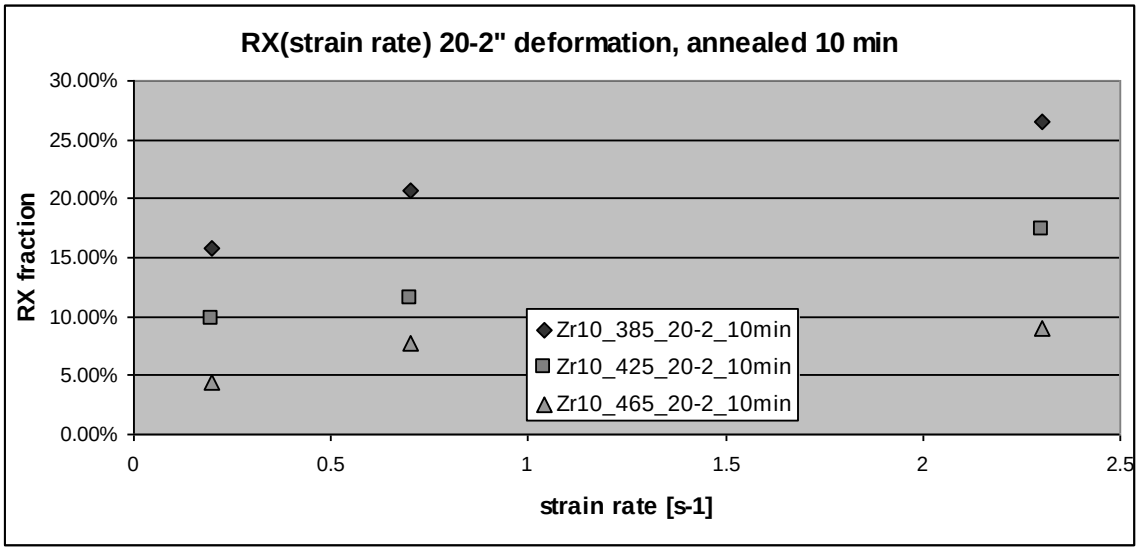

Figure 3.4.2.1b: Recrystallization as a function of strain rate for the plane strain compression tests (annealed at 465°C for 10 minutes).

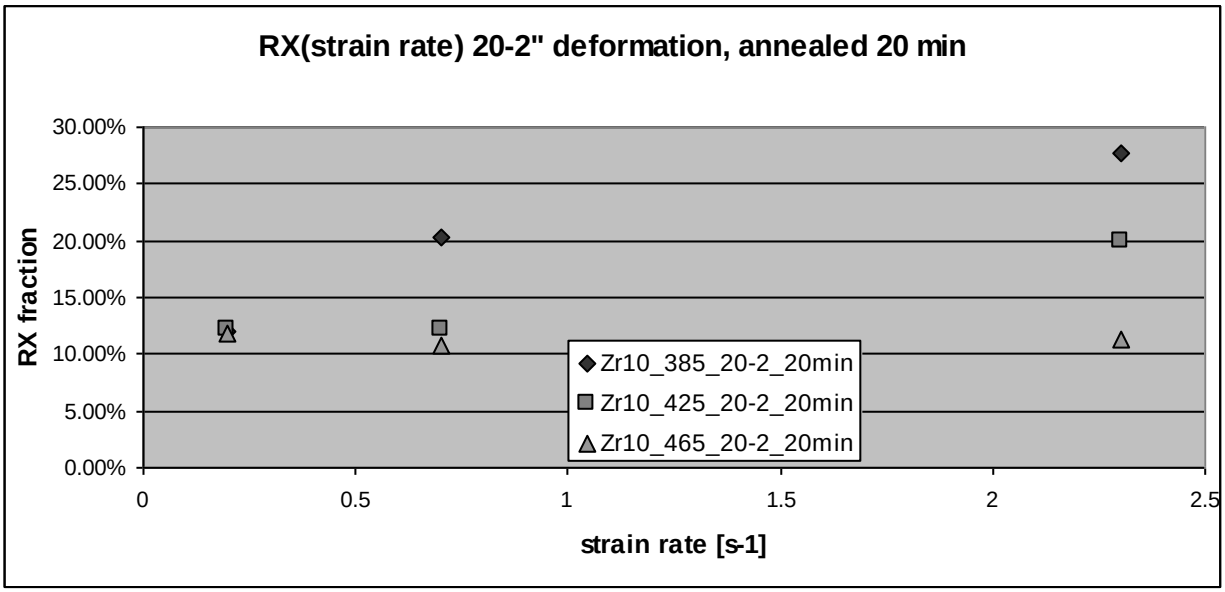

Figure 3.4.2.1c: Recrystallization as a function of strain rate for the plane strain compression tests (annealed at 465°C for 20 minutes). Note: all three data points for the $0.2s^{-1}$-strain rate condition overlap around 12% recrystallization.

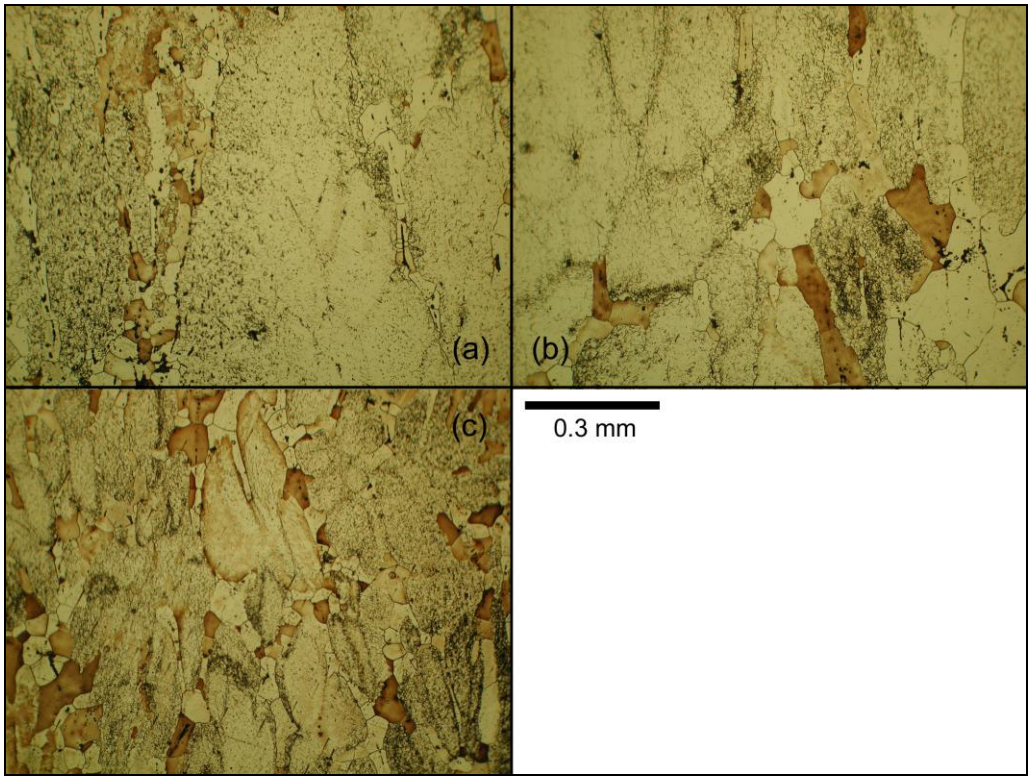

Figure 3.4.2.2: Recrystallization with increasing strain rate for the plane strain compression tests (annealed at 465°C for 10 minutes). Strain rate increases (a) to (c), all other conditions the same. Images taken from Zr10_385_20-2_r02_10min (a), r07_10min (b), r23_10min (c).

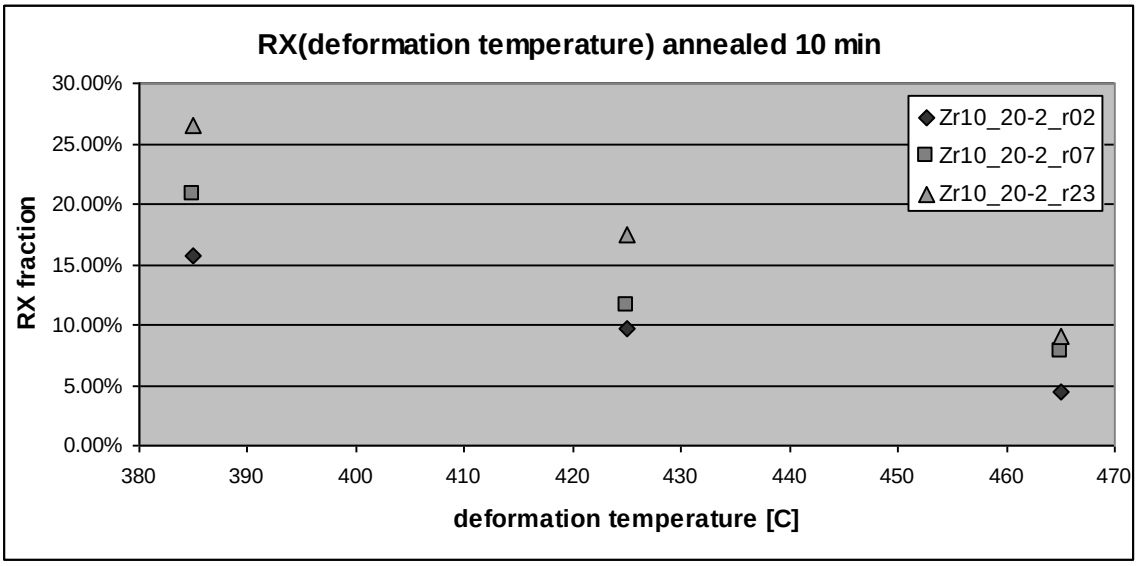

Figure 3.4.3.1a: Recrystallization as a function of deformation temperature for the plane strain compression tests (annealed at 465°C for 10 minutes).

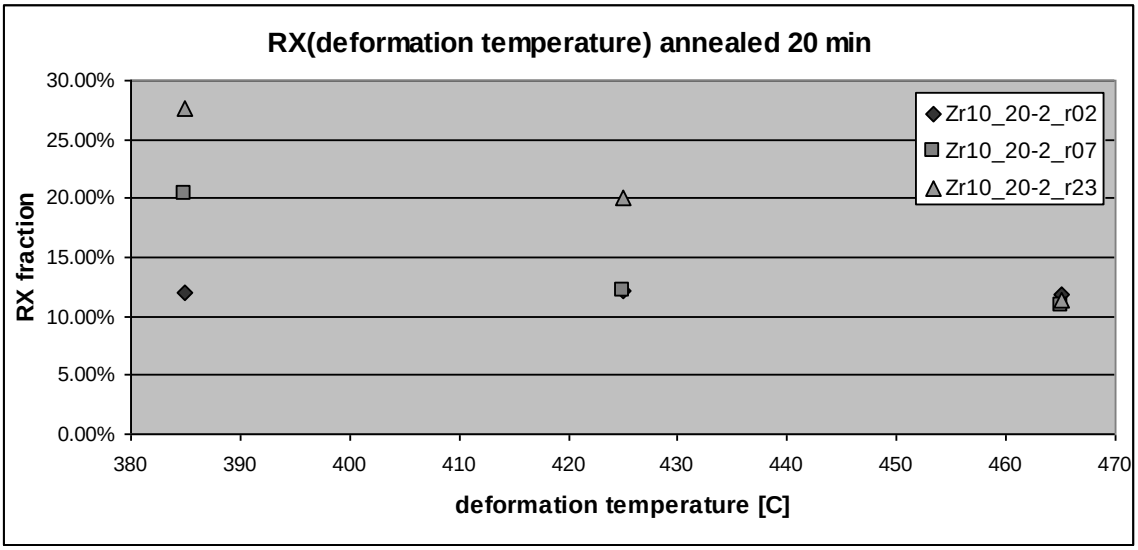

Figure 3.4.3.1b: Recrystallization as a function of deformation temperature for the plane strain compression tests (annealed at 465°C for 20 minutes). Note: all three data points for a deformation temperature of 465°C overlap around 11% recrystallization. For a 425°C deformation temperature, the $0.2s^{-1}$- and $0.7s^{-1}$-strain rate conditions overlap around 12% recrystallization.

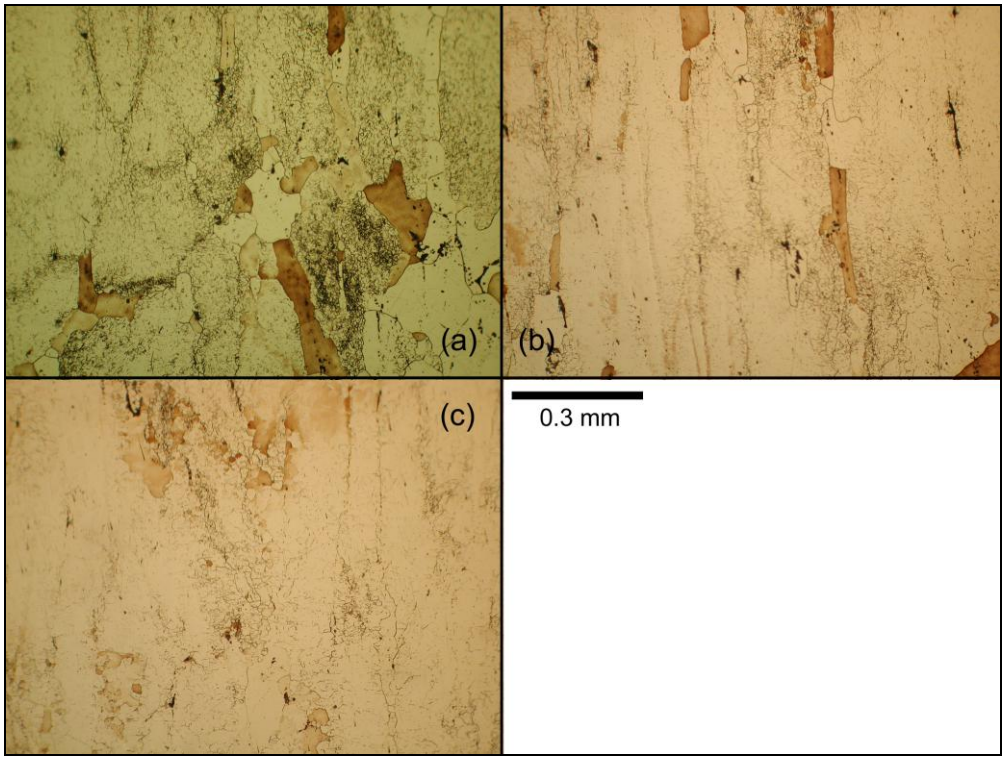

Figure 3.4.3.2: Recrystallization with increasing deformation temperature for the plane strain compression tests (annealed at 465°C for 10 minutes). Deformation temperature increases (a) to (c), all other conditions the same. Images taken from Zr10_385_20-2_r07_10min (a), Zr10_425_20-2_r07_10min (b), Zr10_465_20-2_r07_10min (c).

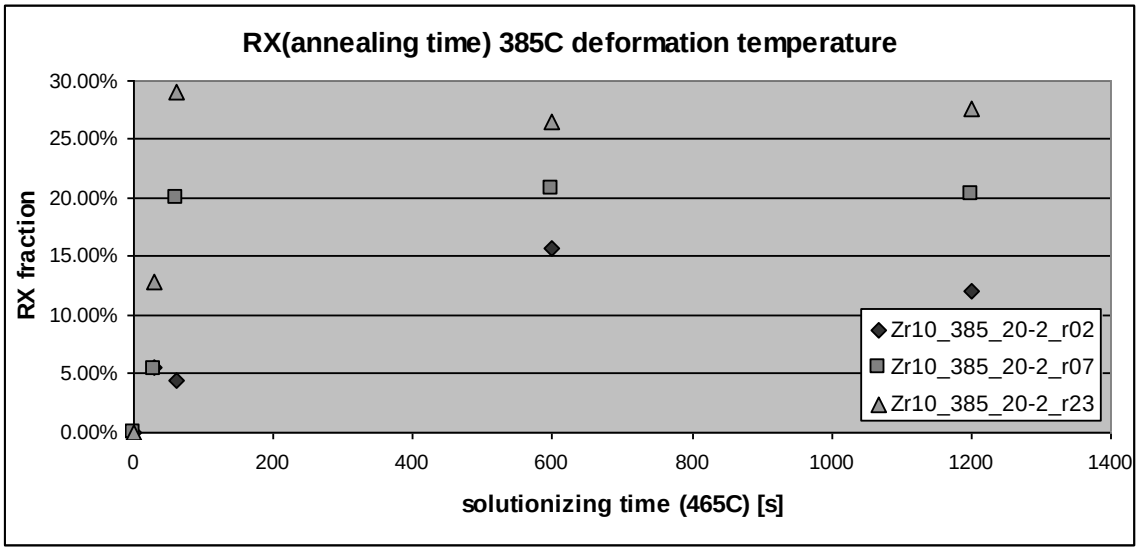

Figure 3.4.4a: Recrystallization as a function of deformation temperature for the plane strain compression tests (deformed to a strain of 0.89 at 385°C). Note: For a annealing time of 30 seconds, the 0.2s-1- and 0.7s-1-strain rate conditions overlap between 5 and 6% recrystallization.

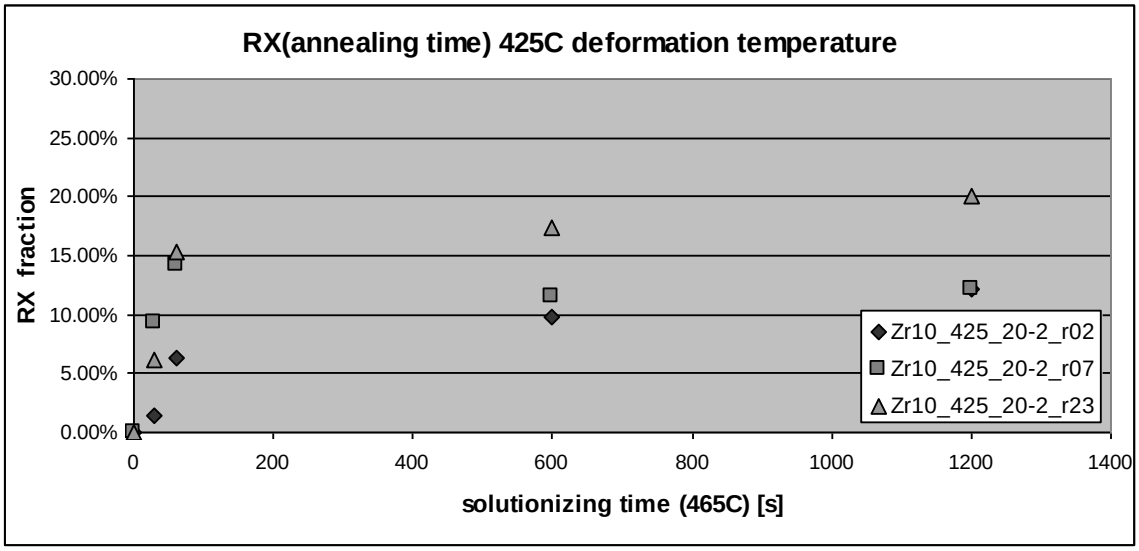

Figure 3.4.4b: Recrystallization as a function of annealing time for the plane strain compression tests (deformed to a strain of 0.89 at 425°C). Note: For an annealing time of 1200 seconds (20 minutes), the 0.2s-1- and 0.7s-1-strain rate conditions overlap around 12% recrystallization.

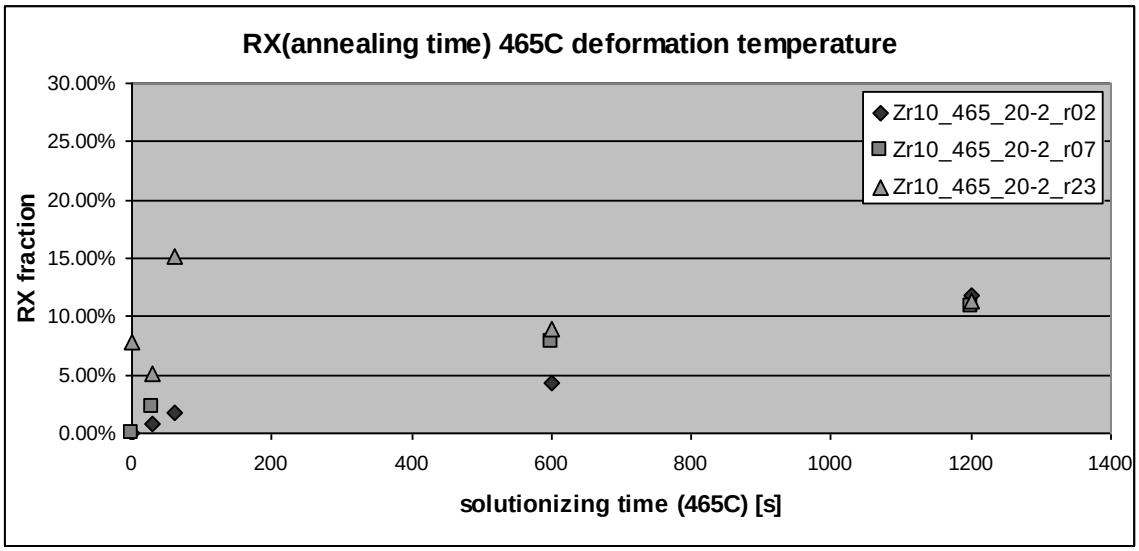

Figure 3.4.4c: Recrystallization as a function of annealing time for the plane strain compression tests (deformed to a strain of 0.89 at 465°C). Note: the data point for Zr10_465_20-2_r07_1min is absent due to damage during the annealing process. No data was collected for this set of conditions. All three data points for a annealing time of 1200 seconds (20 minutes) overlap around 11% recrystallization.

CHAPTER FOUR

CONCLUSIONS

Recrystallization can be controlled in hot-rolled AA 7050 by varying strain, strain rate, deformation temperature, and composition. With increasing strain, more energy is stored in the structure, driving recrystallization. However, for the highly deformed (0.89 strain) and fully annealed (within the range of heat treat times for this experiment) specimens, there appeared to be a minimum amount of recrystallization, approximately 12%. It appears that regardless of deformation conditions, for a given strain, there is a minimum amount of recrystallization due to driving force input by deformation. Any further reduction in recrystallization would require the addition of recrystallization inhibitors, like zirconium.

Reducing strain rate appears to be an effective method to reduce recrystallization. At the lowest strain rate, the recrystallized fraction is the same for all deformation temperatures (for fully annealed, high deformation specimens). It is possible that the low rates allow sufficient time for dynamic recovery, even at low deformation temperatures. As strain rate increases, recrystallization appears to become more sensitive to deformation temperature. Recrystallization increases with increasing strain rate. However, the *rate of increase* of recrystallization with increasing strain rate appears to decrease as strain rates reach higher values. While the recrystallization is sensitive to strain rate, there will be a limit to its effects.

Immediately following strains of 0.79 or higher, at strain rates above 2.3 s-1 at 465°C, there is some RX. However, following any heat treatment, RX follows expected trends with deformation temperature. As the deformation temperature increases, the fraction of recrystallization decreases, likely due to extensive recovery decreasing the driving force for recrystallized grains to

nucleate and grow. With higher deformation temperatures, the influence of strain rate on stored energy may be negated by extensive dynamic recovery such that strain is the only source of stored energy for recrystallization. However, the difference in recrystallized fraction between high and low deformation temperature conditions becomes more pronounced with increasing strain rates.

This data will be used in further work to develop a through-process model simulating structure evolution and deformation conditions throughout hot rolling, allowing processing parameters to be optimized and produce final products with ideal microstructure and properties.

BIBLIOGRAPHY

1. Zhen, L., Hu, H., Wang, X., Zhang, B., Shao, W. “Distribution characterization of boundary misorientation angle of 7050 aluminum alloy after high-temperature compression.” Journal of Materials Processing Technology 209 (2009) pp. 754-761.

2. Field, D.P., Behrens, L., Root, J.M. “Identification of Particle Stimulated Nucleation during Recrystallization of AA 7050.” Computers, Materials, & Continua vol. 1, no.3 (2009) pp. 171-183.

3. Hu, H.E., Zhen, L., Yang, L., Shao, W.Z., Zhang, B.Y. “Deformation behavior and microstructure evolutoin of 7050 aluminum alloy during high temperature deformation.” Materials Science and Engineering A 488 (2008) pp. 64-71.

4. Hu, H.E., Zhen, L., Zhang, B.Y., Yang, L., Chen, J.Z. “Microstructure characterization of 7050 aluminum alloy during dynamic recrystallization and dynamic recovery.” Materials Characterization 59 (2008) pp. 1185-1189.

5. Liu, S., You, J., Zhang, X., Deng, Y., Yuan, Y. “Influence of cooling rate after homogenization on the flow behavior of aluminum alloy 7050 under hot compression.” Materials Science and Engineering ! 527 (2010) pp. 1200-1205.

6. Starke, Jr., E.A., Staley, J.T. “Application of modern aluminum alloys to aircraft.” Prog. Aerospace Sci. Vol. 32 (1995) pp. 131-172.

7. Deng, Y.L., Wan, L., Zhang, Y., Zhang, X-M. “Evolution of microstructures and textures of 7050 Al alloy hot-rolled plate during staged solution heat-treatments.” Journal of Alloys and Compounds 488 (2010) pp. 88-94.

8. Turner, T.J., Miller, M.P., Barton, N.R. “The influence of crystallographic texture and slip system strength on deformation induced shape changes in AA 7050 thick plate.” Mechanics of Materials 34 (2002) pp. 605-625.

9. Daaland, O., Nes, E. “Origin of cube texture during hot rolling of commercial Al-Mn-Mg alloys.” Acta Materialia Vol.4, No. 4 (1996) pp. 1389-201.

10. Robson, J.D., Pragnell, P.B. “Modeling the Variation in Recrystallized Fraction through the Thickness of AA7050 Plate.” Materials Science Forum Vols. 396-403 (2002) pp. 545-550.

11. Xie, F., Yan, Z., Ding, L., Zhang, F., Chen, S., Chu, M.G., Chang, Y.A. “A study of microstructure and microsegregation of aluminum 7050 alloy.” Materials Science and Engineering A 355 (2003) pp. 144-153.

12. Humphreys, F.J., Hatherly, M. *Recrystallization and Related Annealing Phenomena*. 1st ed. Pergamon (1995) pp. 1-415.

13. Robson, J.D. “Microstructural evolution in aluminum alloy 7050 during processing.” Materials Science and Engineering A 382 (2004) pp. 112-121.

14. Robson, J.D., Pragnell, P.B. “Modelling Al3Zr dispersoid precipitation in multicomponent aluminium alloys.” Materials Science and Engineering A352 (2003) pp. 240-250.

15. Jia, Z., Hu, G., Forbord, B., Solberg, J.K. “Effect of homogenization and alloying elements on recrystallization resistance of Al-Zr-Mn alloys.” Materials Science and Engineering A 444 (2007) pp. 284-290.

16. Chakrabarti, D.J., Weiland, H., Cheney, B.A., Staley, J.T. “Through thickness property variations in 7050 plate.” Materials Science Forum Vols. 217-222 (1996) pp. 1085-1090.

17. Talamantes-Silva, J., Abbod, M.F., Puchi Cabrera, E.S., Howard, I.C., Beynon, J.H. “Microstructure modelling of hot deformation of Al-1%Mg alloy.” Materials Science and Engineering A 525 (2009) pp. 147-158.

18. Wong, S.F., Hodgson, P.D., Chong, C.J., Thomson, P.F. “Physical modelling with application to metal working, especially hot rolling.” Journal of Materials Processing Technology 62 (1996) pp. 260-274.

19. Sellars, C.M., Zhu, Q. “Microstructural modelling of aluminium alloys during thermomechanical processing.” Materials Science and Engineering A280 (2000) pp. 1-7.

20. Hosford, W.F. *Physical Metallurgy*. Taylor and Francis (2005) pp. 53-212.

21. Robson, J.D. “Optimizing the homogenization of zirconium containing commercial aluminium alloys using a novel process model.” Materials Science and Engineering A 338 (2002) pp. 219-229.

22. Totik, Y., Gavgali, M. “The effect of homogenization treatment on the hot workability between the surface and the center of AA 2014 ingots.” Materials Characterization 49 (2003) pp. 261-268.

23. Dieter, G.E. *Mechanical Metallurgy*. 3rd ed. McGraw-Hill (1986) pp. 503-615.

24. Zhang, H., Lin, G.Y., Peng, D.S., Yang, L.B. Lin, Q.Q. “Dynamic and static softening behaviors of aluminum alloys during multistage hot deformation.” Journal of Materials Processing Technology 29 (2004) pp. 245-249.

25 Vandermeer, R.A., Jensen, D.J. “Microstructural path and temperature dependence of recrystallization in commercial aluminum.” Acta Materiala 49 (2001) pp. 2083-2094.

26. Vandermeer, R.A., Juul Jensen, D. “Recrystallization in hot vs cold deformed commercial aluminum: a microstructure path comparison.” Acta Materialia 51 (2003) pp. 3005-3018.

27. Cerri, E., Evangelista, E., Forcellese, A., McQueen, H.J. “Comparative hot workability of 7012 and 7075 alloys after different pretreatments.” Materials Science and Engineering A197 (1995) pp. 181-198.

28. Panchanadeeswaran, S. Field, D.P. “Texture Evolution during plane strain deformation of aluminum.” Acta metall. Mater. Vol. 43, No. 4. (1995) pp.1683-1692.

29. Duckham, A., Knutsen, R.D. “Asymmetric flow during plane strain compression testing of aluminum alloys.” Materials Science and Engineering A 256 (1998) pp. 220-226.